Cotrimoxazole reduces systemic inflammation in HIV infection by modulating the gut microbiota and blunting immune cell activation

Authors: Claire D. Bourke[1*#], Ethan K. Gough[2†#], Godfrey Pimundu[3], Annie Shonhai[4], Chipo Berejena[4], Louise Terry[5], Lucas Baumard[1], Naheed Choudhry[1], Yusuf Karmali[1], Mutsa Bwakura-Dangarembizi[4], Victor Musiime[3,6], Joseph Lutaakome[7], Adeodata Kekitiinwa[8], Kuda Mutasa[9], Alexander J. Szubert[10], Moira J. Spyer[10], Jane R. Deayton[1,5], Magdalena Glass[2], Hyun Min Geum[2], Claire Pardieu[1], Diana M. Gibb[10], Nigel Klein[11], Thaddeus J. Edens[12], A. Sarah Walker[10], Amee R. Manges[2‡] and Andrew J. Prendergast[1,9,10‡]

Affiliations:

[1]Blizard Institute, Queen Mary University of London, London, UK

[2]School of Population and Public Health, University of British Columbia, Vancouver, Canada

[3]Joint Clinical Research Centre, Kampala, Uganda

[4]College of Health Sciences, University of Zimbabwe, Harare, Zimbabwe

[5]Royal London Hospital, Barts Health NHS Trust, London, UK

[6]Makerere University, College of Health Sciences, Department of Paediatrics and Child Health, Kampala, Uganda

[7]Uganda Virus Research Institute/MRC Uganda Research Unit on AIDS, Entebbe, Uganda

[8]Baylor – Uganda, Mulago Hospital, Kampala, Uganda

[9]Zvitambo Institute for Maternal and Child Health Research, Harare, Zimbabwe

[10]MRC Clinical Trials Unit at University College London, London, UK

[11]UCL Great Ormond Street Institute of Child Health, London, UK

[12]Devil's Staircase Consulting, West Vancouver, British Columbia, Canada

Author Notes:

[#]These authors contributed equally to this work.

[‡]These authors contributed equally to this work.

[†]Current affiliations:

Ethan K. Gough: The Johns Hopkins Bloomberg School of Public Health, Baltimore, USA

Magdalena Glass: Canada's Michael Smith Genome Sciences Centre, Vancouver, Canada

*To whom correspondence should be addressed:

Claire D. Bourke, Centre for Genomics and Child Health, Blizard Institute, Barts and the London School of Medicine and Dentistry, Queen Mary University of London, London, U.K; c.bourke@qmul.ac.uk

One Sentence Summary: Long-term cotrimoxazole prophylaxis in HIV infection reduces systemic and intestinal inflammation by suppressing gut-resident Streptococci and modulating immune cell activation.

ABSTRACT

Long-term cotrimoxazole prophylaxis reduces mortality and morbidity in HIV infection but the mechanisms underlying these sustained clinical benefits are unclear. Here we investigate the impact of cotrimoxazole on systemic inflammation, an independent driver of HIV mortality. Using longitudinal plasma samples from HIV-positive Ugandan and Zimbabwean children receiving antiretroviral therapy in the ARROW trial, we show that inflammatory markers were lower after randomization to continue (n=144) versus stop (n=149) cotrimoxazole. This was not explained by clinical illness, HIV disease progression or nutritional status. Since sub-clinical enteropathogen carriage and HIV enteropathy can drive systemic inflammation, we explored the impact of cotrimoxazole on the microbiome and biomarkers of intestinal inflammation using fecal samples from ARROW. Although there were no global differences in microbiome community composition, viridans group Streptococci and streptococcal mevalonate pathway enzymes were lower among children randomized to continue (n=36) versus stop (n=36) cotrimoxazole. These changes were associated with lower levels of fecal myeloperoxidase, a biomarker of mucosal leukocyte activity. To isolate the direct effect of cotrimoxazole on immune activation from its effects on the microbiota, we established *in vitro* models of systemic and intestinal inflammation with and without cotrimoxazole treatment. Cotrimoxazole directly blunted pro-inflammatory cytokine production by blood leukocytes from HIV-positive (n=16) and HIV-negative (n=8) UK adults. It also reduced production of the neutrophil chemoattractant IL-8 by monolayers of inflamed gut epithelial cells. Together, these data demonstrate that cotrimoxazole prophylaxis reduces systemic and intestinal inflammation and that this is likely mediated both indirectly, through its antibiotic effects on the microbiota, and by direct

modulation of immune and epithelial cell activation. Synergy between these pathways may contribute to the sustained clinical benefits of long-term cotrimoxazole prophylaxis despite high antimicrobial resistance, providing a further rationale for extending coverage among people living with HIV in sub-Saharan Africa.

INTRODUCTION

In 2017, 36.9 million people were living with HIV globally and 940,000 died from AIDS-related illnesses(*1*). To reduce mortality and morbidity(*2, 3*), World Health Organization (WHO) guidelines recommend long-term cotrimoxazole prophylaxis for all people living with HIV in areas with a high prevalence of malaria and/or severe bacterial infections, regardless of HIV disease stage, CD4 cell count or use of antiretroviral therapy (ART)(*4*). However, it is unclear why cotrimoxazole continues to effectively reduce mortality and morbidity in the context of high rates of antimicrobial resistance and selection for resistant pathogens with long-term use(*2*). There is therefore a need to better understand the effect of cotrimoxazole on HIV pathogenesis.

Systemic inflammation is independently associated with mortality in HIV infection(*5-7*) and this association is stronger in people living with HIV than among HIV-negative people(*8*). Cotrimoxazole might plausibly confer benefits in HIV infection by reducing inflammatory pathology, either indirectly by targeting pathogens that trigger inflammatory responses, or directly by acting on cells that produce pro-inflammatory mediators. Animal models suggest that other antibiotics confer anti-inflammatory benefits, including reduced monocyte activation and cytokine production in SIV-infected minocycline-treated macaques(*9*), and observational studies of HIV-positive adults in high-income settings suggest that cotrimoxazole can reduce levels of plasma inflammatory biomarkers(*10, 11*). Data from randomized trials and low-income settings are lacking and no studies have evaluated the direct and indirect effects of cotrimoxazole on pro-inflammatory pathways in

people living with HIV.

HIV drives a chronic enteropathy, characterized by loss of villous architecture, increased permeability, mucosal CD4+ T-cell depletion(*12*), leukocyte infiltration(*13-15*), and microbial translocation(*16-18*), accompanied by increased pathogen carriage and an altered microbiome(*19-22*); together, these changes contribute to systemic inflammation(*16, 19, 23*). Cotrimoxazole prophylaxis could influence intestinal inflammation indirectly through antibiotic effects on gut pathogens and/or the microbiome, or directly by affecting mucosal leukocytes and gut epithelial cells(*24, 25*). Among HIV-positive Ugandan adults cotrimoxazole was found to have limited effects on the gut microbiota(*23*), however the effects of continuing cotrimoxazole on microbiota composition or HIV enteropathy have not been assessed in a randomized trial or in children.

Cotrimoxazole comprises two folate pathway inhibitors, trimethoprim and sulfamethoxazole. The hypothesis that cotrimoxazole can directly alter the pro-inflammatory responses of circulating immune cells was first posited in 1970, following the observation that intramuscular trimethoprim effectively prolonged skin graft retention in mice to the same extent as the structurally similar immunosuppressive drug azathioprine(*26*). However, subsequent *in vitro* studies of the direct effects of cotrimoxazole on innate and adaptive immune cells have yielded conflicting results(*27-32*) and none have assessed its anti-inflammatory effects on cells from HIV-positive individuals. Cotrimoxazole treatment of rats also impacts absorption across the gut epithelium(*24*), suggesting that cotrimoxazole may

influence gut barrier function, a critical regulator of cross-talk between circulation and gut-resident microorganisms.

Thus, cotrimoxazole prophylaxis confers long-term clinical benefits in HIV infection, which are not entirely explained by its antibiotic effects(*2*, *3*). Inconsistent evidence suggests that cotrimoxazole may have anti-inflammatory properties, but conclusive data are lacking, particularly among children living with HIV in low-income settings. We therefore capitalized on a randomized trial of continuing versus stopping cotrimoxazole in HIV-positive children in sub-Saharan Africa, to test the hypothesis that cotrimoxazole reduces systemic inflammation. We then explored mechanistic pathways through which this may occur using a combination of clinical data, stored specimens and *in vitro* models.

RESULTS

Cotrimoxazole reduces systemic inflammation in HIV-positive children

We have previously shown that randomization to continue compared to stopping cotrimoxazole prophylaxis reduced hospitalization or death among HIV-positive children on long-term ART in the ARROW trial in Uganda and Zimbabwe(*33*). Since inflammatory biomarkers such as CRP and IL-6 are independently associated with mortality in HIV infection, including in the ARROW cohort(*5*), we hypothesized that the benefits of cotrimoxazole might be partly mediated through reductions in systemic inflammation. Inflammatory biomarkers (CRP, IL-6, soluble (s)CD14 and TNFα) were quantified in longitudinal cryopreserved plasma samples from children randomized to continue (n=144) versus stop (n=149) cotrimoxazole within ARROW (**Fig. 1**).

Biomarkers were similar between groups at baseline (**Fig. 1A-D**), but subsequent CRP concentrations from week-24 until the end of follow-up were lower in children randomized to continue cotrimoxazole (**Fig. 1A**). IL-6 was also significantly lower among children continuing cotrimoxazole, particularly at early time-points (**Fig. 1B**). There was no evidence of global differences between groups in sCD14 (**Fig. 1C**) or TNFα (**Fig. 1D**). Plasma albumin was significantly higher (median: 42 versus 41g/L, p=0.041) and total protein significantly lower (76 versus 78g/L, p=0.038) in children continuing cotrimoxazole when measured at week-48 (**Fig. 1E**), consistent with less systemic inflammation. Collectively these results show definitively, through the randomized design, that cotrimoxazole reduces systemic inflammation in HIV-positive children.

To estimate the clinical implications of these differences, we used our previously reported relative risk estimates of adverse outcomes (defined as death, new or recurrent World Health Organization clinical stage 4 events, or poor immunological response to ART) associated with pre-ART pre-cotrimoxazole levels of CRP and IL-6 in ARROW(*5*). Stopping cotrimoxazole in the current analysis led to increases in CRP and IL-6 levels at week-24 of 1.65-fold (stop 2.71mg/L versus continue 1.64mg/L; **Figure 1A**) and 1.18-fold (stop mean: 5.36pg/mL versus continue 4.54pg/mL; **Figure 1B**) respectively. Based on the previous ARROW model for adverse outcomes this would correspond to an increased relative risk among children stopping cotrimoxazole of 13% (95% CI: 4-24%) and 11% (95% CI: 4-18%) within 24 weeks(*5*). Relative differences in CRP, which were maintained between randomized groups throughout follow-up, peaked at week-48 (1.92-fold increase; 2.86mg/L stop versus 1.49mg/L continue; **Figure 1A**), corresponding to an 18% (95% CI: 6-32%) increased risk of adverse clinical outcomes. Thus, the cotrimoxazole-mediated differences that we observed in CRP and IL-6 levels are clinically relevant to long-term survival, health and immune restoration among children living with HIV.

Reduced systemic inflammation is not solely due to reduced clinical infections

One explanation for reduced systemic inflammation among children continuing cotrimoxazole prophylaxis would be an improved course of their HIV infection due to reductions in intercurrent infections, particularly common but less severe infections not leading to hospitalization or death(*2, 33*). However, there was no evidence of global differences in the proportion of children with viral suppression (<80 HIV RNA copies/mL;

106 **Fig. 2A**) or in CD4+ T-cell percentages (%CD4; **Fig. 2B**) between randomized groups. There
107 was also no evidence of differences between randomized groups in caregiver-reported cough
108 (**Fig. 2C**), fever (**Fig. 2D**), nausea/vomiting (**Fig. 2E**) or abdominal pain (**Fig. 2F**) across the
109 whole follow-up period or at individual time-points, with the exception of fever at week-12
110 (7.4% continue versus 20.2% stop, p=0.01). Too few children had persistent, bloody or
111 moderate-to-severe diarrhea, difficult/fast breathing and/or weight loss for comparison
112 between groups. Thus, although the ARROW trial found that continuing cotrimoxazole
113 reduced hospitalization or death(*33*), effects of cotrimoxazole on systemic inflammation were
114 not explained by differences in HIV disease progression or symptomatic infections between
115 groups.

116

117 ***Cotrimoxazole prophylaxis does not affect nutritional status***

118 HIV-positive children frequently have malnutrition, and antibiotics (including cotrimoxazole)
119 have been shown to improve growth(*34*) and slow weight-loss(*35*). We therefore compared
120 anthropometry between randomized groups, reasoning that differences in systemic
121 inflammation might be explained by underlying wasting or stunting(*36, 37*). We found no
122 evidence of differences between groups in weight-for-age (**Fig. 2G**) or height-for-age Z-
123 scores (**Fig. 2H**), suggesting that lower inflammatory biomarkers were not driven by
124 improved nutritional status in children continuing cotrimoxazole.

125

126 ***Cotrimoxazole alters circulating CD4+ T-cell phenotype in HIV-positive children***

127 Although continuation of cotrimoxazole had no impact on total CD4 counts (**Fig. 2B)**, we

hypothesized that CD4+ T-cell phenotypes would differ between randomized groups. Elevated systemic inflammation is frequently accompanied by T-cell activation in HIV infection(*38*, *39*) and we have previously shown that pre-ART pre-cotrimoxazole percentages of proliferating (Ki67+) CD4+ T-cells are positively associated with systemic inflammation in the ARROW cohort(*5*). T-cell immunophenotyping was conducted via flow cytometry in a subset of Ugandan ARROW participants to determine the effects of cotrimoxazole on T-cell activation and differentiation (stop n=48, continue n=47; **fig. S1A**). There was no evidence for a difference between groups in the proportions of total CD4+ T-cells expressing the activation marker HLA-DR or the proliferation marker Ki67 (**fig. S1B-C**). Children continuing cotrimoxazole had higher percentages of recent thymic emigrant-like cells (RTE, CD4+CD45RA+CD31+ T-cells; an indicator of thymic output(*40*)) than children stopping prophylaxis (**fig. S1B**). There was no evidence of difference in proportions of naïve (CD4+CD45RA+CD31-) and effector-memory (CD4+CD45RA-CD31-) T-cells or in the expression of HLA-DR on any CD4+ T-cell sub-populations (**fig. S1C**). However, children continuing cotrimoxazole had a lower percentage of proliferating (Ki67+) RTE and naïve T-cells, particularly at later time-points post-randomization (**fig. S1D**); this did not correspond to differences in mature or total CD4+ T-cells. Thus, cotrimoxazole prophylaxis is associated with shifts in the composition and mobilization of the circulating T-cell pool, consistent with reduced systemic inflammation(*5*).

Long-term cotrimoxazole suppresses fecal Streptococci but not Enterobacteriaceae

Microbial consortia in the gut are disrupted by HIV infection, which contributes to local and systemic inflammation(*21, 41*). Although we found no difference between randomized

153 groups in symptomatic intercurrent infections (**Fig. 2C-F**), we hypothesized that continuing
154 cotrimoxazole would drive sustained sub-clinical differences in gut pathogens and
155 commensals. We conducted whole metagenome shotgun sequencing of total fecal DNA from
156 children randomized to continue (n=36 at week-84; n=33 at week-96) versus stop
157 cotrimoxazole (n=36 at week-84; n=35 at week-96), compared bacterial community
158 dissimilarity between randomized groups using the Bray–Curtis index and visualized this
159 with non-metric multidimensional scaling (NMDS) plots (**Fig. 3A** and **B**). Hypothesis testing
160 by permutation indicated no significant difference in community composition between
161 children randomized to continue versus stop cotrimoxazole at either week-84 (**Fig. 3A**) or
162 week-96 (**Fig. 3B**). However, zero-inflated beta regression analysis of microbiome
163 characteristics identified seven bacterial species (*Alistipes onderdonkii, Eggerthella lenta,*
164 *Clostridium bartlettii, Haemophilus parainfluenzae, Streptococcus mutans, Streptococcus*
165 *parasanguinis* and *Streptococcus vestibularis*; **fig. S2**) and 11 protein families (Pfam; **fig.**
166 **S3**), which mapped to *Streptococcus parasanguinis*, *Streptococcus salivarius* and
167 *Haemophilus parainfluenzae*, that were consistently less abundant at both time-points in
168 samples from children continuing versus stopping cotrimoxazole (relative abundance ratio
169 <1) after FDR adjustment. The cotrimoxazole-affected Streptococcal species, all part of the
170 Viridians group of Streptococci (VGS), largely fell in the quadrant of the NMDS ordination
171 plot where the extremes of the treatment groups lay (**Fig. 3A** and **B**).

172

173 The relative abundance of Enterobacteriaceae, which includes common gastrointestinal
174 pathogens (e.g. *Salmonella*, *Escherichia coli*, and *Shigella*) that are frequently resistant to
175 cotrimoxazole(*42-44*), was not affected by cotrimoxazole at week-84 (relative abundance

ratio: 0.65, adjusted-p=0.108) and was increased in those continuing versus stopping cotrimoxazole at week-96 (4.48, adjusted-p<0.001).

To confirm the specific differences that we observed in VGS abundance according to cotrimoxazole we conducted high-resolution mapping of metagenome sequencing reads to Streptoccoci pangenome datasets using PanPhlAn software. PanPhlAn has a lower false positive rate for species-level identification and a better discrimination between samples containing the same versus different bacterial genomes than the MetaPhlAn software used for all bacterial species(*45*). Of the 140 fecal samples sequenced (both groups at week-84 and week-96), PanPhlAn identified 29 samples that were positive for the presence of any Streptococci (9 species were present: *S. salivarius, S. parasanguinis, S. mutans, S. vestibularis, S. australis, S. infantarius, S. oligofermentans, S. pasteurianus,* and *S. sanguinis*) and, of these, 20 samples that were positive for at least one of the 4 VGS species identified as being suppressed by cotrimoxazole using MetaPhlAn (7 at week-84 and 13 at week-96). Compared to MetaPhlAn, PanPhlAn identified a lower percentage of VGS-positive samples on account of its higher species-level resolution (**Fig. 3D** and **E**). Six samples from children continuing and 14 samples from children stopping cotrimoxazole were confirmed to be VGS-positive across both timepoints, corroborating VGS suppression by cotrimoxazole. Individual VGS species were confirmed to be present less often in children continuing cotrimoxazole (**Fig. 3E**); *S. salivarius* was found most frequently (6 continue samples versus 12 stop samples), followed by *S. vestibularis* (3 versus 10 samples), *S. parasanguinis* (1 versus 3 samples) and *S. mutans* (0 versus 2 samples) across both timepoints; **Fig. 3E**.

Together, these findings show that continuing cotrimoxazole among HIV-positive children treated with ART and cotrimoxazole for a median of 2 years prior to randomization does not have additive effects on global microbiome community composition. However, continuation of cotrimoxazole does drive specific alterations in fecal microbiome characteristics, with suppression of VGS confirmed at species-level resolution but no evidence for sustained increases on sub-clinical carriage of Enterobacteriaceae.

Cotrimoxazole suppresses the Streptococcal mevalonate pathway

To understand the effect of cotrimoxazole on functional pathways within the differentially abundant fecal microbiome species, we investigated microbial metabolic function by quantifying the abundance of the full set of genes in a metabolic pathway regardless of the taxa encoding them. Of the metabolic pathways, only mevalonate pathway I, which influences neutrophil and monocyte recruitment and function(*46*, *47*), was consistently different according to cotrimoxazole treatment at both time-points. The abundance of mevalonate pathway-associated genes was significantly lower in fecal samples from children continuing cotrimoxazole (**Fig. 3C**). Of the enzyme-encoding genes within mevalonate pathway I, those with identity to *Streptococcus parasanguinis* and *Streptococcus salivarius* were significantly less abundant in the continue group (**Fig. 3C**).

Overall our fecal microbiome analyses identified a metagenomic signature of mevalonate metabolism in VGS that is reduced with long-term cotrimoxazole prophylaxis (summarized in **Fig. 3C**; analyses of all bacterial species and Pfam in **fig. S2** and **S3**, respectively).

Cotrimoxazole-induced changes in fecal Streptococci are associated with reduced intestinal inflammation

We next tested whether or not the cotrimoxazole-driven changes to microbiota composition and function influenced HIV enteropathy. We first compared levels of fecal inflammatory markers from a sub-set of Zimbabwean ARROW children with stored stool samples at week-84 and week-96 post-randomization to continue (n=37) or stop (n=38) cotrimoxazole. We chose myeloperoxidase, neopterin, alpha-1 antitrypsin and regenerating gene 1β (REG1β) as biomarkers of neutrophil and monocyte activity, macrophage and dendritic cell activation, gut permeability, and epithelial turnover, respectively(*48*). At week-84, fecal myeloperoxidase was significantly lower in children continuing versus stopping cotrimoxazole (median: 1694ng/mL versus 3178ng/mL, p=0.022; **Fig. 4A**), but there was no evidence of differences in neopterin, alpha-1-antitrypsin, or REG1β between groups (p>0.15, **fig. S4A**). At week-96, fecal myeloperoxidase tended to be lower in children continuing cotrimoxazole (1262 versus 1473ng/mL, p=0.093; **Fig. 4B**), but there was no evidence of differences in neopterin, alpha-1-antitrypsin or REG1β between groups (p>0.15, **fig. S4B**). Since myeloperoxidase is an abundant peroxidase enzyme in monocytes and neutrophils that perpetuates granulocyte activation(*49*) and both monocytes and neutrophils home to the gut mucosa during HIV infection(*14*, *15*), these observations suggest that cotrimoxazole reduces innate immune cell activity in the gut.

Of the bacterial species suppressed by cotrimoxazole, *Streptococcus mutans*, *Streptococcus vestibularis*, *Streptococcus parasanguinis*, and *Haemophilus parainfluenzae* were positively associated with myeloperoxidase levels at week-96 (*Streptococcus* spp. summarized in **Fig.**

248 **4C**; analysis of all cotrimoxazole-affected species is shown in **fig. S5**), after adjustment for
249 age, sex, and cotrimoxazole group. Myeloperoxidase levels were also positively associated
250 with Pfam that were differentially abundant according to cotrimoxazole treatment, 5 with
251 identity to *Streptococcus parasanguinis*, 2 to *Streptococcus salivarius*, 2 to *Haemophilus*
252 *parainfluenzae*, and 1 to *Eubacterium bioforme* at week-96 (Pfam with identify to
253 *Streptococcus* spp. summarized in **Fig. 4C**; analysis of all cotrimoxazole-affected Pfam is
254 shown in **fig. S6**). Overall mevalonate pathway I abundance was significantly associated with
255 higher myeloperoxidase at week-96 and tended towards a positive association at week-84
256 (**Fig. 4C**). Of the mevalonate pathway I enzymes that differed between randomized groups,
257 only those with identity to *Streptococcus parasanguinis* and *Streptococcus salivarius* had a
258 significant positive association with myeloperoxidase (**Fig. 4C**).

259

260 We therefore show that all VGS components suppressed by cotrimoxazole (**Fig. 3C**) were
261 also significantly positively associated with myeloperoxidase at week-96 (**Fig. 4C**),
262 suggesting that sub-clinical effects of cotrimoxazole on VGS abundance and function
263 contribute to lower intestinal inflammation among children continuing cotrimoxazole.

264

265 ***Cotrimoxazole blunts pro-inflammatory cytokine responses in vitro***

266 Having established that continuation of cotrimoxazole reduces both systemic and intestinal
267 inflammation among HIV-positive children on ART, we next investigated whether
268 cotrimoxazole has direct immunomodulatory properties. In order to isolate any direct effects
269 of cotrimoxazole on immune cells from its impact on the microbiota, we optimized an *in vitro*

model of whole blood cytokine responses to bacterial and fungal antigens: heat-killed *Salmonella typhimurium* (HKST), which activates immune cells via Toll-like receptor (TLR) 2, 4 and 5; purified *Escherichia coli* lipopolysaccharide (LPS), which engages TLR4; and the *Saccharomyces cerevisiae* cell-wall component zymosan, which engages TLR2 and dectin-1. Antigens that engage innate pathogen recognition receptors were chosen for these assays to reflect the elevated microbial translocation reported during HIV infection, which drives systemic inflammation and immune activation(*7*, *16*, *19*, *41*). Cotrimoxazole dose was chosen to reflect maximum (high-dose; 8µg/mL trimethoprim and 200µg/mL sulfamethoxazole) and minimum (low-dose; 2µg/mL trimethoprim and 50µg/mL sulfamethoxazole) serum concentrations in HIV-positive patients taking cotrimoxazole(*50*). Laboratory cotrimoxazole preparations were confirmed to have antibiotic activity (**fig S7A**) and had no impact on cell viability at the concentrations used for subsequent experiments (**fig. S7B-D**).

Since systemic inflammation can affect subsequent immune cell responses to stimuli, we predicted that the *in vitro* effects of cotrimoxazole might be influenced by the pre-existing inflammatory milieu. We therefore obtained blood samples from cotrimoxazole-untreated HIV-positive (ART-treated (n=6) and ART-naïve (n=10)) and HIV-negative UK adults (n=8, **table S1**) with confirmed differences in baseline systemic inflammation, circulating monocytes, and T- cell activation (**fig. S8**). There was no difference between the groups in spontaneous cytokine production in unstimulated cultures over 24h (**Fig. 5**).

Treatment with high-dose cotrimoxazole significantly reduced levels of HKST-, LPS- and

zymosan-induced TNFα **(Fig 5A**) and IL-6 (**Fig 5B**) relative to control treatment with drug diluent alone (DMSO) in one or more group. This was particularly evident for HKST- and LPS-induced TNFα and LPS- and zymosan-induced IL-6, which were significantly lower across all three clinical groups. LPS- and zymosan-induced TNFα and zymosan-induced IL-6 were also significantly reduced by low-dose cotrimoxazole in the HIV-positive ART-naïve group (**Fig 5A** and **B**).

These observations confirm our hypothesis that cotrimoxazole directly modulates pro-inflammatory immune cell activation by pathogen antigens, both in HIV-positive and in HIV-negative individuals independently of the effect of oral cotrimoxazole prophylaxis on microbiome composition or intestinal inflammation.

Cotrimoxazole affects monocyte but not T-cell cytokine production

To determine the immune cell types modulated by cotrimoxazole, we evaluated intracellular TNFα production and surface expression of HLA-DR by monocytes and T-cells during 6h PBMC culture with or without high-dose cotrimoxazole. Cotrimoxazole reduced the proportion of TNFα+ monocytes after HKST stimulation relative to control-treated cultures in the HIV-negative group but not in the HIV-positive groups (**Fig. 5C**). Cotrimoxazole did not alter HKST-induced up-regulation of HLA-DR by monocytes (**Fig. 5C**). Cotrimoxazole also had no effect on the proportion of TNFα+ or HLA-DR+ CD4+ or CD8+ T-cells after polyclonal stimulation with staphylococcal enterotoxin B (SEB; **Fig. 5D** and **E**). Thus, although cotrimoxazole reduces pro-inflammatory cytokine production by blood leukocytes

317 and TNFα production by monocytes specifically, it does not directly reduce monocyte
318 maturation or T-cell activation as assessed by HLA-DR expression.

319

320 ***Cotrimoxazole reduces IL-8 production by gut epithelial cells***

321 The gut epithelium provides a barrier between the microbiota and gut mucosal immune cells,
322 responds to TLR ligands, and produces leukocyte chemoattractants under inflammatory
323 conditions; direct effects of cotrimoxazole on epithelial cell function could contribute to its
324 anti-inflammatory effects. To isolate direct effects of cotrimoxazole on the epithelial barrier
325 from its impact on the microbiota, we used transwell cultures of the Caco-2 human colonic
326 epithelial cell-line as a well-established model of gut epithelium. We induced epithelial
327 inflammation with IL-1β and evaluated the effect of cotrimoxazole on four epithelial
328 functions that could influence cross-talk between microbes and mucosal immune cells:
329 epithelial integrity (trans-epithelial resistance, TEER), epithelial cell death (%Lactose
330 dehydrogenase (LDH) activity), apical-to-basal translocation of a fluorescent dye (%Lucifer
331 Yellow passage, a proxy for microbial translocation), and production of the neutrophil
332 chemoattractant IL-8 (**Fig. 6A**). We used higher cotrimoxazole concentrations for these
333 experiments than for whole blood cultures to reflect the higher concentrations found in the
334 gut lumen following oral dosing, after first titrating cotrimoxazole in Caco-2 cultures to
335 identify a dose that did not differ in cytotoxicity from DMSO controls (1mg/mL; **Fig. 6B**).

336

337 Cotrimoxazole treatment throughout Caco-2 growth did not significantly alter the rate of
338 monolayer confluence (mean TEER/plate >800Ω; **Fig. 6C**), ΔTEER, %LDH activity or

340 %Lucifer yellow passage under inflammatory conditions relative to DMSO control-treatment
341 (1, 10 or 100µg/mL IL-1β for 24h; **Fig. 6D**). However, cotrimoxazole-treated monolayers
342 produced significantly less IL-8 than control-treated cultures when the inflammatory stimulus
343 was highest (100µg/mL IL-1β, p=0.003) and tended to produce less IL-8 at lower IL-1β
344 concentrations than DMSO-treated cultures (1µg/mL, p=0.257, and 10µg/mL, p=0.095; **Fig.**
345 **6D**).

346

347 Taken together, these experiments suggest that cotrimoxazole can directly modulate IL-8
348 production by gut epithelial cells independently of its effects on the microbiome, which may
349 contribute to reduced neutrophil recruitment to the intestinal mucosa under inflammatory
350 conditions.

DISCUSSION

Inflammation drives morbidity and mortality among people living with HIV. There is therefore growing interest in identifying adjunctive anti-inflammatory agents to improve clinical outcomes with ART(*51-54*). Cotrimoxazole is currently recommended long-term for children and adults living with HIV in settings with high prevalence of malaria or invasive bacterial infections, although global coverage remains poor(*4*, *55*). We show here that long-term continuation of cotrimoxazole prophylaxis reduces systemic inflammation in ART-treated children living with HIV in sub-Saharan Africa and demonstrate several novel mechanisms through which this may occur, including antibiotic effects on the fecal microbiome and direct anti-inflammatory effects on leukocyte and gut epithelial cell cytokine production *in vitro*. Synergy between antibiotic and anti-inflammatory pathways may explain the sustained clinical benefits of cotrimoxazole for people living with HIV in settings where the prevalence of cotrimoxazole-resistant pathogens is high(*3*, *33*) and provides an additional rationale for improving coverage of cotrimoxazole prophylaxis in sub-Saharan Africa.

We first exploited available samples from the ARROW trial, allowing us to show definitively, using the randomized stop-versus-continue design, that the systemic inflammatory biomarkers CRP and IL-6 are reduced by cotrimoxazole. We also observed cotrimoxazole-mediated changes in serum proteins and circulating naive CD4+ T-cell mobilization consistent with reduced systemic inflammation. Whilst it would be desirable in future studies to include more comprehensive infection screening, we found no evidence for differences in caregiver-reported symptoms of intercurrent illnesses between the

randomized groups. We therefore reasoned that the long-term benefits of continuing cotrimoxazole may be partially mediated through its anti-inflammatory effects. Previous studies have demonstrated that, even with very early initiation of ART, not all circulating inflammatory mediators are normalized when HIV viremia is controlled(*56*, *57*) and high levels of certain inflammatory mediators continue to predict morbidity and mortality(*5-7*, *58*). We have previously shown that pre-ART pre-cotrimoxazole levels of both CRP and IL-6, but not TNFα or sCD14, predicted the relative risk of three important clinical outcomes (mortality, WHO stage 4 clinical events and poor CD4 reconstitution) in the ARROW trial; a 2-fold increase in baseline CRP or IL-6 was independently associated with 19% and 54%, increased risk of these outcomes, respectively(*5*). Absolute mortality rates are lower among HIV-positive children after initiating ART and cotrimoxazole; however, based on our predictions from pre-ART biomarker levels, the reductions in CRP and IL-6 that we demonstrate among children continuing cotrimoxazole in the current study would reduce their relative risk of adverse outcomes over the subsequent 24 weeks post-randomization by 13% and 11%, respectively compared to children who stopped cotrimoxazole. These estimates highlight that the anti-inflammatory benefits of cotrimoxazole are clinically meaningful, and may have substantial impact at a population level, given the ultimate goal of universal coverage of cotrimoxazole among people living with HIV.

Soluble inflammatory mediators appear to be better predictors of poor clinical outcomes than T-cell activation among people living with HIV in resource-limited settings(*8*). In a subgroup of children in Uganda, we were able to evaluate the impact of cotrimoxazole on T-cell immunophenotype. We observed lower percentages of proliferating naïve CD4+ T- cells

among children continuing cotrimoxazole, which we interpret as a beneficial phenotype since elevated CD4+ T-cell proliferation without a corresponding increase in total counts is associated with depletion of the naïve T-cell pool(*59*). Unfortunately, ARROW sample limitations meant that our analysis of circulating immune cell activation was limited to HLA-DR expression on CD4+ T-cells, for which we did not identify an effect of continuing cotrimoxazole. To more comprehensively assess the effects of *in vivo* cotrimoxazole on immune cells, future studies should include a wider range of T-cell surface activation markers and assessment of CD8+ T-cell and innate immune cell activation.

We went on to explore the underlying factors driving the cotrimoxazole-mediated differences in circulating CRP and IL-6. Systemic inflammation in HIV infection is partly driven by enteropathogen carriage and chronic enteropathy(*12-14, 16*) and the effect of cotrimoxazole on these domains has not been previously characterized. Using fecal samples from a sub-set of children randomized within ARROW, we demonstrated that VGS were less abundant in children continuing prophylaxis at both week-84 and week-96 post-randomization. Since speciation of VGS can be challenging, we confirmed the species-level differences that we observed according to cotrimoxazole using high-resolution mapping of metagenome sequencing reads to Streptococcal pangenomes databases(*45*). These analyses confirmed that *S. salivarius*, *S. vestibularis*, *S. parasanguinis* and *S. mutans* were specifically suppressed by cotrimoxazole. The effects of cotrimoxazole on VGS are particularly striking since global microbiome community composition did not significantly differ between randomized groups, likely because these children had been receiving cotrimoxazole with ART for a median of 2 years prior to randomization(*33*). VGS are a heterogeneous group of bacteria, which can

423 be both commensal and pathogenic(*60*); they are frequently observed in the oral microbiome,
424 but are found throughout the healthy human gut(*61, 62*). VGS are also enriched in fecal
425 samples from children with stunting(*63*), a form of chronic malnutrition associated with
426 elevated systemic inflammation(*64*), suggesting that so-called 'decompartmentalization' of
427 microbial communities along the gastrointestinal tract and immune activation may be
428 interrelated. For example, VGS express a range of immune-stimulatory antigens, and potently
429 activate innate immune cell cytokine production *in vitro*(*65*). In contrast to changes in VGS,
430 we found no evidence for suppression of Enterobacteriaceae, a taxonomic group including
431 pathogens causing severe bacterial infections among people living with HIV, which are
432 frequently resistant to cotrimoxazole in sub-Saharan Africa(*42-44*). Thus, whilst sub-clinical
433 carriage of Enterobacteriaceae might be expected to drive systemic inflammation, this did not
434 appear to be the case in this cohort. Our microbiome analyses focused on later time-points
435 post-randomization, due to sample availability; there may therefore have been additional
436 antibiotic effects of cotrimoxazole at earlier time-points and other anatomical sites, which we
437 were not able to investigate.

438

439 We went on to explore the relationship between cotrimoxazole-mediated changes in the
440 microbiota and biomarkers of intestinal inflammation. Children randomized to continue
441 cotrimoxazole had lower levels of fecal myeloperoxidase, an antimicrobial peroxidase
442 enzyme abundantly expressed in neutrophil granules and a biomarker of enteropathy, which
443 was associated with a number of microbiota characteristics. Of the cotrimoxazole-affected
444 VGS, *Streptococcus mutans, Streptococcus parasanguinis* and *Streptococcus vestibularis*
445 were positively associated with fecal myeloperoxidase levels. Myeloperoxidase more readily

447 kills group A and group B streptococci than VGS *in vitro*(*66*). Thus, VGS may have a
448 selective advantage over more myeloperoxidase-susceptible species in HIV enteropathy,
449 during which myeloperoxidase-producing innate leukocytes accumulate in the gut(*15*, *67*).
450 Our data indicate that these novel sub-clinical antibiotic effects of cotrimoxazole on VGS
451 contribute to reduced intestinal inflammation. A recent study of experimentally induced
452 suppression of gram-positive bacteria in rhesus macaques with vancomycin prior to SIV
453 infection, indicated that antibiotic-induced dysbiosis was not associated with differences in
454 IL-6 or CD4+ T cell activation in the mesenteric lymph nodes relative to SIV infection
455 alone(*68*). Thus, the timing of antibiotic treatment (before SIV infection in macaques and
456 after HIV infection in humans), existing microbiota composition, history of ART treatment,
457 intercurrent infection prevalence and antibiotic specificity all likely influence the relationship
458 between antibiotic-induced changes in the microbiota and intestinal inflammation.

459

460 Our microbiome analyses highlighted bacterial gene markers of mevalonate pathway I,
461 predominantly mapping to VGS, which decreased with cotrimoxazole continuation and were
462 positively associated with fecal myeloperoxidase. The mevalonate pathway is one of two
463 metabolic processes that produce isoprenoids, a diverse class of naturally occurring organic
464 precursors in eukaryote cholesterol synthesis and prokaryote cell wall peptidoglycan (a TLR2
465 ligand)(*69*). Several *in vitro* studies indicate that inhibition of mevalonate pathway
466 components impairs innate leukocyte recruitment and function, providing a precedent for
467 how inhibition of VGS mevalonate metabolism by cotrimoxazole might influence HIV
468 enteropathy. For example, inhibiting farnesyl pyrophosphate synthesis reduces neutrophil
469 priming by IL-8(*70*), and inhibiting hydroxymethylglutaryl-CoA reductase (HMG-CoA)

activity reduces IL-6 and IL-8 production by monocytes(*71*) and trans-epithelial migration by neutrophils(*51, 54*). HMG-CoA with identity to *Streptococcus parasanguinis* and *Streptococcus salivarius* was among the mevalonate pathway enzymes that we found to be less abundant in children continuing cotrimoxazole. Given these observations, our data suggest that cotrimoxazole prophylaxis in HIV-positive children may reduce innate leukocyte recruitment and activation in the gut indirectly by suppressing VGS and their myeloperoxidase-promoting mevalonate pathway.

Leukocytes are an abundant source of pro-inflammatory cytokines, which are synthesized and released following ligation of innate pathogen recognition receptors including TLRs. Multiple studies have demonstrated higher levels of circulating microbial products that could trigger these pathways during HIV infection, including the TLR4 ligand LPS(*11, 16*). We developed an *in vitro* model of leukocyte activation by TLR ligands to isolate direct anti-inflammatory effects of cotrimoxazole from its antibiotic effects on pathogenic and commensal microbes, using blood samples from HIV-negative and HIV-positive UK adults who were not receiving cotrimoxazole. Physiologically relevant cotrimoxazole doses had a consistent inhibitory effect on *in vitro* whole blood TNFα and IL-6 production elicited via TLR2, 4 and 5 signaling, suggesting that modulation of innate pro-inflammatory cytokine production is a property of cotrimoxazole *per se*, and occurs independently of its antibiotic properties, pre-existing inflammation or ART exposure. Intracellular cytokine staining of PBMC suggested that monocyte rather than T-cell cytokine production was most affected by cotrimoxazole, albeit less consistently than the effect seen on whole blood cytokine responses. Our demonstration of direct modulation of pro-inflammatory cytokine production

by blood leukocytes clarifies a longstanding theory that cotrimoxazole modulates immune responses in mice via an undefined mode-of-action(*26*), for which subsequent studies have yielded opposing conclusions using *in vitro* models of innate(*27-29*, *31*, *32*) and adaptive(*28*, *30*, *31*) immune cell function. Most existing studies were conducted several decades ago and used inconsistent immunoassays; our study has the advantage of more recent functional immunology assays and was informed by the ARROW trial findings, which highlighted pro-inflammatory cytokine production as a clinically relevant pathway(*5*). The *in vitro* effects observed were quantitatively subtle; however, our prior analysis of pre-ART IL-6 levels in plasma from ARROW suggest that small differences are independently associated with reduced relative risk of adverse clinical outcomes among HIV-positive children(*5*). Additional studies are necessary to characterize the pharmacology of cotrimoxazole-mediated immunosuppression, the nature of its interaction with TLR signaling and evaluate its potential therapeutic value in other inflammatory disorders. Our observations in UK adults provide a rationale for further exploration of the effects of cotrimoxazole on innate and adaptive immune cell function in HIV-positive and HIV-negative children.

Using a separate *in vitro* model we found that long-term cotrimoxazole treatment also reduced production of the neutrophil chemoattractant IL-8 by inflamed epithelial cells. This is a novel putative pathway through which cotrimoxazole could directly contribute to reduced neutrophil recruitment and myeloperoxidase production in the gut mucosa during HIV enteropathy. Cotrimoxazole did not alter epithelial characteristics associated with barrier function (epithelial integrity, dye translocation or cell viability) *in vitro*. However, it remains possible that these pathways are altered *in vivo* through drug effects on components of the

gut barrier, such as the mucus layer(*24*) and expression of tight junction proteins(*68*), which we did not model. Biopsy specimens were not available from children in ARROW; however, evaluation of the effect of cotrimoxazole on gut biopsies from HIV-positive donors and *in vitro* using 3-dimensional gut models, which more accurately mimic trans-epithelial transport, would be desirable for extending this work. Since VGS express abundant TLR2 ligands and the Caco-2 line express low levels of TLR2(*72*), alternative epithelial cell lines or primary epithelial cells with intact TLR2 signaling would be required to explore the relevance of cotrimoxazole-mediated changes to VGS metabolism to epithelial barrier function in *vitro*.

Collectively, this study identifies cotrimoxazole as an immunomodulator as well as an antibiotic, which reduces both systemic and intestinal inflammation in HIV infection. We have identified an anti-inflammatory agent that has the advantage of being routinely recommended with ART in sub-Saharan Africa, widely available, well-tolerated and low-cost(*2*). Our study raises the possibility that antibiotics other than cotrimoxazole may confer anti-inflammatory benefits that contribute to their impact at scale in low-income settings, for example the recent demonstration of reduced child mortality following mass administration of azithromycin(*73*). The potential for antibiotics to have accessory benefits to direct pathogen killing, contributes to current debate around antibiotic stewardship in settings where antimicrobial resistance is already high and particularly for conditions such as HIV, where chronic inflammation combines with intercurrent infection to exacerbate clinical outcomes. Whether or not cotrimoxazole has clinical benefits for people living with HIV in high-income countries, where long-term prophylaxis is not currently recommended, warrants further study

542

543 since ART alone does not fully prevent pathology. The demonstration of its anti-

544 inflammatory benefits in this study should drive renewed efforts for universal cotrimoxazole

545 coverage to improve clinical outcomes for all people living with HIV in sub-Saharan Africa.

MATERIALS & METHODS

Ethical approval

The Antiretroviral Research for Watoto trial (ARROW; ISRCTN Registry# ISRCTN24791884; http://www.isrctn.com/ISRCTN24791884) and use of biological specimens collected from children enrolled in ARROW were approved by Research Ethics Committees in Uganda, Zimbabwe, and the UK. Written informed consent from all caregivers and assent from participants, where appropriate, was obtained as previously described(*33*, *74*).

Approval to assess the effect of *in vitro* cotrimoxazole on immune cell activation in adult volunteers with and without HIV infection was provided by the UK National Health Service Research Authority (NHS IRAS project ID: 209553; Research Ethics Council reference: 17/WM/0018) and the Research Ethics Committee of Queen Mary University of London. All participants provided written informed consent.

ARROW randomized trial

Cryopreserved plasma and fecal samples were obtained from children enrolled in ARROW, an open-label, randomized, parallel-group trial among HIV-positive children. One randomization within ARROW recruited children and adolescents (median age: 7.9 years, interquartile range (IQR): 4.6, 11.1) who had been receiving ART for >96 weeks in the trial (median duration of ART: 2.1 years, IQR: 1.8, 2.2) at medical centers in Uganda (Joint Clinical Research Centre, Kampala; Baylor College of Medicine Children's Foundation,

569

570 Mulago Hospital, Kampala; MRC/UVRI Uganda Research Unit on AIDS, Entebbe) and
571 Zimbabwe (University of Zimbabwe, Harare)(*33, 74*). At baseline all participants were
572 receiving once-daily cotrimoxazole prophylaxis (200mg of sulfamethoxazole and 40mg of
573 trimethoprim, 400mg of sulfamethoxazole and 80mg of trimethoprim, or 800mg of
574 sulfamethoxazole and 160mg of trimethoprim for a body weight of 5-15, 15-30, or >30 kg,
575 respectively).

576

577 Participants were randomly assigned to stop (n=382) or continue (n=386) daily cotrimoxazole
578 prophylaxis as previously described(*33, 74*). Children were seen in clinic every 6 weeks to
579 record caregiver-reported symptoms of infection since the previous visit and measure height
580 and weight. CD4 count was measured and plasma stored (including for retrospective HIV
581 viral load testing) every 12 weeks post-randomization to a common trial end date (16th March
582 2012). Children were excluded from the original ARROW trial (for which ART was initiated
583 at enrolment) if they did not meet the 2006 WHO criteria for ART initiation(*75*), had acute
584 infections, had previously received ART or were perinatally exposed to ART (children <6
585 months old), were pregnant or breastfeeding, or were taking medications or had laboratory
586 abnormalities that contraindicated ART(*74*). Children were excluded from the subsequent
587 randomization to stop versus continue cotrimoxazole if they had a history of *Pneumocystis*
588 *jirovecii* pneumonia(*33*). 98% of children enrolled into ARROW during the last 6 months of
589 the recruitment period were also included in an immunology sub-study(*5*), and additional
590 assays were conducted for samples from these children as well as from a random 23% sample
591 of all remaining non-immunology sub-study children, as previously described(*5*).

592

Inclusion of children from the ARROW randomization trial and immunology sub-study in the current study was determined by country of recruitment and sample availability, specified for each sample-type below.

Circulating biomarker quantification

CRP, TNFα, IL-6 and sCD14 were quantified via ELISA (Quantikine kits; R&D Systems Inc.) in children with available plasma samples who were enrolled into the immunology sub-study of ARROW in Uganda and Zimbabwe, and in all other children randomized to stop versus continue cotrimoxazole in Zimbabwe. All children who had baseline measurements (i.e. at randomization to stop versus continue cotrimoxazole) were included in statistical comparisons between randomized groups at 12, 24, 48, 72 and 96 weeks post-randomization, using the closest available measurement to each study time-point in equally spaced windows (stop n=149 versus continue n=144).

For children known to have fasted for >6 hours prior to sample collection, total protein was analyzed in one serum sample per child collected at week-48 post-randomization to stop (n=151) or continue (n=159) cotrimoxazole (+/- 24 weeks; equivalent to 3 years after enrolment to the ARROW trial and ART initiation). Albumin, and total protein were quantified using a Beckman CX5 Delta Chemistry Analyzer (Beckman Coulter) as previously described(*76*).

ARROW clinical symptoms

Longitudinal caregiver-reported clinical symptoms since the last study visit (6-week recall of incidents of cough, fever, abdominal pain/aching, nausea/vomiting, persistent, bloody or moderate-to-severe diarrhea, difficult/fast breathing and weight loss), weight-for-age and height-for-age Z scores were compared between the stop (baseline n=150) versus continue (baseline n=145) groups for children who were also included in the plasma biomarker quantification assays.

Immunophenotyping of blood leukocytes

Fresh whole blood was used to undertake T-cell immunophenotyping by flow cytometry in the sub-set of ARROW children enrolled in the immunology sub-study in Uganda only and for whom blood sample volumes were sufficient (stop n=48 versus continue n=47), as previously described(*5*). Leukocytes were labelled with the following fluorophore-conjugated antibodies: CD4-PerCP (BD Biosciences), CD31-PE (eBiosciences) and CD45RA-APC (Caltag Medsystems) and Ki67-FITC (BD Biosciences; staining performed after membrane permeabilization). Cell phenotyping was conducted on a BD FACSCalibur flow cytometer and analyzed using CellQuest software (BD Biosciences; gating strategy is shown in **fig. S1A**).

Fecal inflammatory marker quantification

Fecal samples were collected from children enrolled in the ARROW immunology sub-study and randomized to stop (n=38) or continue (n=37) cotrimoxazole in Zimbabwe only at week-84 and week-96 of follow-up. Myeloperoxidase, neopterin, α1-antitrypsin, and REG1β were

quantified in cryopreserved fecal samples using ELISA kits from Immun diagnostik AG, Genway Biotech Inc, Immuchrom GmbH, and Techlab Inc, respectively.

Fecal DNA preparation and sequencing

Total DNA was extracted from week-84 and week-96 150 mg fecal samples from 72 children enrolled in the ARROW immunology sub-study in Zimbabwe (Stop n=36, Continue n=36) using the MoBio DNA Extraction Kit with bead-beating modified for simultaneous RNA isolation. Paired-end DNA libraries were prepared using Illumina® TruSeq® Nano DNA Library Prep kits. As a quality control, the libraries were analyzed on a TapeStation 2200 before pooling. Whole metagenome sequencing was performed with 125-nucleotide paired-end read lengths using the Illumina HiSeq 2500 platform at Canada's Michael Smith Genome Sciences Centre, Vancouver, Canada. 23-24 libraries were pooled per sequencing lane.

Sequenced reads were trimmed of adapters and filtered to remove low-quality, short (<60 base-pairs), and duplicate reads, as well as those of human, other animal or plant origin using KneadData with default settings. Species composition was determined by identifying clade-specific markers from reads using MetaPhlan2 with default settings(*77*). Functional gene and metabolic pathway composition was determined using HUMANn2 with default settings against the UniRef90 database(*78*). Functionally annotated reads were further classified into Pfam protein families(*79*) and level-4 enzyme commission (EC) categories using provided scripts. Microbiome species, gene and pathway abundance were normalized by the total read count in each stool sample (relative abundance). Median 10,507,352 versus 11,068,280

662

663 (p=0.23) reads were obtained at week-84, and 11,074,046 versus 10,875,436 (p=0.60) at
664 week-96 from continue and stop groups, respectively.

665

666 ***Microbiome analyses***

667 Alpha diversity was calculated at the species level using the inverse Shannon diversity index,
668 which provides a measure of the effective species number per fecal sample. Differences in
669 species relative abundance and diversity between randomized groups were evaluated at each
670 time-point by intention-to-treat analysis using linear regression models fitted against natural
671 log-transformed inverse Shannon diversity indices. Species diversity did not differ between
672 randomized groups at either visit (13.1 versus 14.3, p=0.27 and 13.5 versus 14.8, p=0.72).
673 Pielou's index of species evenness also showed no difference between randomized groups at
674 week-84 (mean 0.59 versus 0.60 in continue versus stop, p=0.605) or week-96 (mean 0.60
675 versus 0.61 in continue versus stop, p=0.883). Species-level beta diversity was evaluated
676 using the Bray–Curtis dissimilarity index, and visualized using NMDS.

677

678 Differences in species, Pfam, metabolic pathway and enzyme (microbiome characteristic)
679 relative abundance were evaluated at each time point by intention-to-treat analysis using
680 zero-inflated beta regression models fitted against relative abundances. Zero-inflated beta
681 regression is a two-part model with a logistic component to model the presence or absence of
682 each microbiome characteristic, and a beta component to model the non-zero relative
683 abundance, given that a microbiome characteristic is present. This model has been shown to
684 outperform other methods for identifying differentially abundant microbiome characteristics,

in terms of power and false discovery rate (FDR), due to its flexibility for handling non-normal abundances with a large number of zeros(*80, 81*). Zero-inflated beta regression models were fitted using generalized additive models for location, scale and shape with a log-link(*82*), where the variance of the beta distribution was modeled as a function of sequencing depth. Treatment effect was the ratio of relative microbiome characteristic abundance in the continue group versus the stop group. A separate model was fit for each microbiome characteristic. P-values were adjusted for multiple comparisons to maintain the FDR at the desired significance level (α=0.05)(*83*). Only differentially abundant microbiome characteristics that were statistically significant at both week-84 and week-96 after FDR adjustment were interpreted as causally related to long-term cotrimoxazole use. To determine which species were responsible for the observed changes in functional composition, differentially abundant protein families were further stratified by species, while differentially abundant pathways were further stratified by species and pathway enzymes, and zero-inflated beta-regression models were re-fitted with FDR correction.

We determined whether observed changes in microbiome composition were associated with intestinal inflammation by fitting rank-based regression models against fecal myeloperoxidase concentration adjusted for age, sex, and randomized group, with FDR adjustment for multiple comparisons. In these analyses the week-84 and week-96 samples were investigated independently.

To confirm species-level analyses in MetaPhlAn, PanPhlAn was used to pairwise map 140

ARROW datasets to 20 available Streptococcus pangenome databases in order to determine the presence or absence of Streptococcus species at higher sensitivity(*45*). Default settings for the programs panphlan_map.py and panphlan_profile.py were used(*45*).

All microbiome data analyses were conducted in *R* version 3.3.2. The package *VEGAN*(*84*), was used to calculate the Shannon diversity and Bray-Curtis dissimilarity and NMDS. *Gamlss* was used for zero-inflated beta regression(*82*). *Rfit* was used for rank-based regression(*85*).

HIV-negative and HIV-positive UK adult participants

HIV-negative adults were recruited via email circular to research staff at the Blizard Institute, Queen Mary University of London, UK (n=8). HIV-positive adults on ART for >2 years (n=6) or who were ART-naïve (n=10) were identified from outpatient records by clinicians and nurses at the Grahame Hayton Unit of the Royal London Hospital, UK and invited to participate during routine clinical appointments. Participants taking cotrimoxazole or other antibiotics or with clinical signs of intercurrent infections were excluded from the study. After written informed consent was provided, a 50 mL venous blood sample was collected into sterile heparinized blood collection tubes (BD Biosciences) from each participant via venipuncture. 10 mL of blood was used for immunophenotyping and whole blood culture. PBMC and undiluted plasma were isolated from 40 mL of whole blood using Ficoll Plaque Plus (GE Healthcare) density separation. Plasma samples were aliquoted and stored in endotoxin-free cryovials (Greiner) at -80^{0}C. Freshly isolated PBMC were washed twice in

sterile PBS/1% v/v Fetal Bovine Serum (FBS; Gibco) prior to staining and/or culture.

Plasma biomarker quantification

Plasma CRP, sCD14, TNFα (Duoset kits from R&D Systems) and IL-6 (OptEIA kit from BD Biosciences) were quantified in all UK adult participants by ELISA.

Immunophenotyping of uncultured PBMC

$1x10^6$ freshly isolated PBMC were incubated for 30 min with fluorophore-conjugated antibodies specific for T-cell and monocyte surface markers for 30 min (**table S2**), washed once in PBS/1% FBS and fixed for 30 min in Fixation buffer (eBiosciences). Labelling with fluorescence-minus-one (FMO) and isotype control antibodies for each surface marker and a membrane impermeable viability dye (Zombie aqua Fixable Viability dye; Biolegend) were conducted in parallel to determine hierarchical gating (gating strategy shown in **fig. S9B**). Immunophenotyping was conducted for all UK adult participants on a BD LSR II flow cytometer and analyzed using FlowJo LLC software version 10.

Antigens

Lyophilized heat-killed *Salmonella typhimurium* (HKST), ultrapure lipopolysaccharide from *Escherichia coli* 0111:B4 strain (LPS), *Saccharomyces cerevisiae* cell wall (zymosan), and *Staphylococcus aureus* enterotoxin B (SEB; Sigma) were reconstituted according to the manufacturer's instructions.

Drugs

Trimethoprim and sulfamethoxazole were prepared in DMSO at a stock concentration of 100 mg/mL (all from Sigma). Commercially available cotrimoxazole (100 mg/mL; Sigma) pre-formulated in DMSO was used for Caco-2 experiments. Drugs were titrated and assessed for antibiotic activity against bacterial isolates (**fig. S7A**), toxicity to cultured cells (**fig. S7B-D**; **Fig. 7B**), and optimal culture duration (**fig. S7E**) and timing of treatment relative to antigen stimulus (**fig. S7F**) prior to use in cell culture experiments. Controls for each cotrimoxazole treatment dose were prepared using DMSO without drug at the same total volume (i.e. volume of trimethoprim + volume of sulfamethoxazole). Final DMSO content in cultures were 0.05% v/v for $CTX_{[Low]}$ and $DMSO_{[Low]}$ controls and 0.2% v/v for $CTX_{[High]}$ and $DMSO_{[High]}$ controls.

Whole blood culture

Whole blood culture conditions for *in vitro* cotrimoxazole treatment were optimized using samples from HIV-negative adults (n=6; **fig. S7B, C, E** and **F**). Drug and antigen conditions for whole blood culture were batch-prepared in RPMI 1640 GlutaMAX™ (Gibco) supplemented with 1% v/v Penicillin-streptomycin (P-S; Gibco) and stored at -80^0C. Single-use aliquots of drug and antigen conditions were thawed for each donor and combined with 500 µL/well of 1:3 diluted blood (final concentrations in culture: blood at 1:6, HKST at 10^8 cells/mL, LPS at 5 EU/mL, and Zymosan at 5 µg/mL; low-dose cotrimoxazole ($CTX_{[Low]}$): 2 µg/mL trimethoprim and 50 µg/mL sulfamethoxazole, high-dose cotrimoxazole ($CTX_{[High]}$): 8 µg/mL trimethoprim and 200 µg/mL sulfamethoxazole). Whole blood cultures were

incubated for 24h at 37^0C, 5% CO_2 after which cell-free supernatants were harvested and stored at -80^0C. Cytokines in culture supernatants from all UK adults were quantified via sandwich ELISA (TNFα, R&D Duoset ELISA kits and IL-6, BD OptEIA ELISA Kits).

6h PBMC culture

Drug and antigen conditions for PBMC culture were batch-prepared in RPMI 1640 GlutaMAX™/1% P-S/10% FBS (cRPMI) and stored at -80^0C. Single-use aliquots of drug and antigen conditions were thawed for each donor and combined with $1x10^6$ PBMC in 50µL cRPMI with 100µl of pre-prepared drug condition (High dose $CTX_{[High]}$ or volume-matched DMSO control), 50µl of pre-prepared antigen and 50µL cRPMI in sterile round-bottomed tubes (BD Biosciences). Final antigen concentrations in culture were: HKST at 10^8 cells/ mL and SEB at 1µg/mL. PBMC cultures were incubated at 37^0C, 5% CO_2. Brefeldin A (Sigma) was added to all cultures at a final concentration of 25µg/mL after 1h incubation. After a total of 6h culture, PBMC were washed in sterile PBS/1% FBS, labelled with fluorophore-conjugated antibodies specific for cell surface markers (**table S2**) for 30 min, washed in PBS/1% FBS and fixed overnight in fixation buffer (eBiosciences) at 4^0C. Fixed cells were permeabilized in 1x Permeabilization buffer (eBiosciences) and labelled with fluorophore-conjugated antibodies specific for intracellular cytokines (**table S2)** for 40 min, washed once with Permeabilization buffer and once with PBS/1% FBS prior to analysis on a BD LSR II flow cytometer alongside FMO and isotype control-labelled samples (gating strategy shown in **fig. S9**). Analysis was conducted using FlowJo LLC software version 10.

Caco-2 transwell culture

The human colonic epithelial cell-line Caco-2 derived from colorectal adenocarcinoma (ATCC® HTB-37™) was maintained in DMEM (Lonza) supplemented with 1% v/v P-S, 1%v/v L-glutamine, 1% v/v Non-essential amino acids, and 10% v/v FBS (cDMEM; all supplements from Gibco) in 75cm^2 culture flasks at 37^{0}C, 5% CO_2. Cells were passaged on reaching 80-90% confluency using Trypsin/EDTA (Gibco). Experiments were conducted using Caco-2 between passage 35 and 40. Transwell cultures were conducted using 24-well culture plates with Millicell Hanging Cell Culture Inserts (PET 0.4 μm; Merck-Millipore) seeded apically with 1x10^4 cells/well and cultured at 37^{0}C, 5% CO_2. cDMEM was replaced after the first 3 days of culture and every 2 days thereafter. TEER across the growing monolayer was monitored daily using an STX04 test electrode with a Millicell® ERS-2-ohm meter (Merck-Millipore). 1 mg/mL of cotrimoxazole, volume-matched DMSO or cDMEM without drug was added apically to Caco-2 monolayers from the first day post-seed and replenished at each media change during cell growth. Stimulation of the monolayers was conducted when the plate mean TEER was >800Ω, which occurred between day 7-10 post-seeding; individual wells with TEER <600Ω (i.e. sub-confluent) were excluded. Transwells were stimulated apically with 1, 10 or 100 μg/mL recombinant human IL-1β (BioVision Inc) or cDMEM without stimulus for 24h.

Caco-2 functional assays

24h after stimuli were added, TEER was re-recorded and change in TEER calculated (ΔTEER = 24h TEER - pre-treatment TEER), apical supernatants were harvested and stored

at -20^{0}C and Caco-2 monolayers were washed once with sterile pre-warmed PBS and transferred to new 24-well culture plates containing 1 mL/well sterile PBS pre-warmed to 37^{0}C. 100 µg/mL Lucifer Yellow Biocytin dye (Molecular Probes) prepared in sterile pre-warmed PBS was added to the apical side of each transwell and plates were incubated on a plate shaker (100 rpm) at 37^{0}C, 5% CO_2 for 1h. Fluorescence intensity (FI) was quantified in apical and basal culture supernatants relative to an 11-point Lucifer Yellow standard curve (100 – 0.1 µg/mL) using a BioTek plate reader (excitation/emission wavelength: 480/530nm); %Lucifer Yellow apical-to-basal passage = $(FI_{Basal} - FI_{PBS}) / (FI_{100\mu g/\ mL} - FI_{PBS})$.

LDH activity and IL-8 were quantified in cryopreserved apical supernatants using LDH Cytotoxicity Assay Kit (Pierce) and Human IL-8/CXCL8 DuoSet ELISA Kit (R&D Systems) respectively. Apical supernatants from parallel Caco-2 transwell cultures treated with cell lysis buffer (LDH_{Max}; Pierce) or an equivalent volume of sterile endotoxin-free ultrapure water ($LDH_{Spontaneous}$) acted as controls for the LDH assay. LDH activity in drug-treated cultures was calculated: $\%LDH = (LDH_{CTX} - LDH_{Spontaneous}) / (LDH_{Max} - LDH_{Spontaneous}) \times 100$.

Statistical analysis

For ARROW trial data, fold-change in geometric means between randomized groups were compared for continuous variables (CRP, sCD14, IL-6 and TNFα in plasma; weight-for-age and height-for-age Z scores; % CD4+ T-cells and their subsets) at each study time-point using standard regression models and globally across all time-points using generalized estimating equations (GEE; normal distribution for log transformed values), both with

adjustment for recruitment centre and baseline values, and assuming variation in treatment effect by time-point. Proportions of children with HIV-1 viral load <80 copies/mL (viral suppression) were compared between randomized groups at each time-point using Exact tests and globally across all time-points using GEE (binomial distribution) with adjustment for recruitment centre and assuming variation in treatment effect by time-point. Relative risk projections for CRP and IL-6 differences between randomized groups were calculated from the output of models based on pre-ART pre-cotrimoxazole biomarker levels in the ARROW immunology sub-cohort, which we have previously reported(*5*). GEE and Exact tests were conducted in STATA Software version 15.1 (StataCorp LLC). Concentrations of fecal inflammatory markers at week-84 and week-96 and circulating proteins and lipids at week-48 post-randomization (Shapiro Wilk test for normality, $p<0.05$) were compared between randomized groups using the Mann-Whitney U test in Prism version 7.02 Software (GraphPad).

For the *in vitro* cotrimoxazole treatment study, continuous variables (cytokine concentrations and cell proportions; Shapiro-Wilk test for normality, $p<0.05$) were compared between clinical groups (HIV-negative, HIV-positive ART-treated and HIV-positive ART-naïve) using unpaired Kruskall-Wallis tests. Comparisons between drug treatments were only conducted where the response variable was significantly up-regulated in antigen-stimulated cultures without drug treatment versus un-stimulated cultures without drug treatment, i.e. cells were significantly activated to produce cytokines by the stimulus (paired Wilcoxon test, $p<0.05$). Comparisons between drug treatments were made within clinical groups using Freidman tests with post-hoc pair-wise comparisons made using uncorrected Dunn's

869

870 tests; post-hoc tests were only conducted where the global test was statistically significant to
871 limit multiple comparisons.

872

873 Functional read-outs from Caco-2 cultures (TEER, ΔTEER, % LDH activity, % Lucifer
874 Yellow passage and IL-8 levels; Shapiro-Wilk test for normality, $p>0.05$) were compared
875 between cotrimoxazole and DMSO-treated cultures using paired two-tailed t-tests. Analyses
876 included a minimum of 3 separate experiments (conducted using separate passages of Caco-
877 2) per culture condition. All analyses of *in vitro* cell culture models were conducted using
878 Prism version 7.02 software (GraphPad).

879

880 **REFERENCES**

881 1. UNAIDS, Fact sheet - Latest global and regional statistics on the status of the AIDS epidemic - July
882 2018. (2018).
883 2. J. A. Church, F. Fitzgerald, A. S. Walker, D. M. Gibb, A. J. Prendergast, The expanding role of co-
884 trimoxazole in developing countries. *The Lancet Infectious Diseases* **15**, 327-339 (2015).
885 3. A. S. Walker *et al.*, Daily co-trimoxazole prophylaxis in severely immunosuppressed HIV-infected
886 adults in Africa started on combination antiretroviral therapy: An observational analysis of the DART
887 cohort. *The Lancet* **375**, 1278-1286 (2010).
888 4. WHO, *Guidelines on post-exposure prophylaxis for HIV and the use of co-trimoxazole prophylaxis for*
889 *HIV-related infections among adults, adolescents and childrenl: Recommendations for a public health*
890 *approach - December 2014 supplement to the 2013 consolidated ARV guidelines*. (WHO Press,
891 Geneva, Switzerland, 2014), pp. 49.
892 5. A. J. Prendergast *et al.*, Baseline inflammatory biomarkers identify subgroups of HIV-infected African
893 children with differing responses to antiretroviral therapy. *Journal of Infectious Diseases* **214**, 226-236
894 (2016).
895 6. L. H. Kuller, R. Tracy, W. Belloso, Inflammatory and coagulation biomarkers and mortality in patients
896 with HIV infection. *PLoS Medicine* **5**, (2008).
897 7. N. G. Sandler *et al.*, Plasma levels of soluble CD14 independently predict mortality in HIV infection.
898 *Journal of Infectious Diseases* **203**, 780-790 (2011).
899 8. P. W. Hunt, S. A. Lee, M. J. Siedner, Immunologic biomarkers, morbidity, and mortality in treated
900 HIV infection. *Journal of Infectious Diseases* **214**, S44-S50 (2016).
901 9. J. H. Campbell *et al.*, Minocycline Inhibition of Monocyte Activation Correlates with Neuronal
902 Protection in SIV NeuroAIDS. *PLoS ONE* **6**, e18688 (2011).
903 10. J. Vesterbacka *et al.*, Kinetics of microbial translocation markers in patients on Efavirenz or
904 Lopinavir/r based antiretroviral therapy. *PLoS ONE* **8**, e55038 (2013).
905 11. J. Vesterbacka, B. Barqasho, A. Haggblom, P. Nowak, Effects of co-trimoxazole on microbial
906 translocation in HIV-1-infected patients initiating antiretroviral therapy. *AIDS Research & Human*
907 *Retroviruses* **31**, 830-836 (2015).
908 12. J. M. Brenchley, T. W. Schacker, L. E. Ruff, CD4+ T cell depletion during all stages of HIV disease
909 occurs predominantly in the gastrointestinal tract. *Journal of Experimental Medicine* **200**, (2004).
910 13. M. Mavigner *et al.*, Altered CD4+ T cell homing to the gut impairs mucosal immune reconstitution in
911 treated HIV-infected individuals. *Journal of Clinical Investigation* **122**, 62-69 (2012).
912 14. K. Allers *et al.*, Macrophages accumulate in the gut mucosa of untreated HIV-infected patients.
913 *Journal of Infectious Diseases*, (2013).
914 15. M. Somsouk *et al.*, Gut epithelial barrier and systemic inflammation during chronic HIV infection.
915 *AIDS* **29**, 43-51 (2015).
916 16. J. M. Brenchley *et al.*, Microbial translocation is a cause of systemic immune activation in chronic HIV
917 infection. *Nat Med* **12**, 1365-1371 (2006).
918 17. A. P. Kourtis *et al.*, Role of intestinal mucosal integrity in HIV transmission to infants through breast-
919 feeding: the BAN study. *Journal of Infectious Diseases* **208**, 653-661 (2013).
920 18. C. Tincati, D. C. Douek, G. Marchetti, Gut barrier structure, mucosal immunity and intestinal
921 microbiota in the pathogenesis and treatment of HIV infection. *AIDS Research & Therapy* **13**, 19
922 (2016).
923 19. S. M. Dillon *et al.*, An altered intestinal mucosal microbiome in HIV-1 infection is associated with
924 mucosal and systemic immune activation and endotoxemia. *Mucosal immunology* **7**, 983-994 (2014).
925 20. G. Dubourg *et al.*, Gut microbiota associated with HIV infection is significantly enriched in bacteria
926 tolerant to oxygen. *BMJ Open Gastroenterology* **3**, e000080 (2016).
927 21. C. A. Lozupone *et al.*, Alterations in the gut microbiota associated with HIV-1 infection. *Cell Host &*
928 *Microbe* **14**, 10.1016/j.chom.2013.1008.1006 (2013).
929 22. D. M. Dinh, G. E. Volpe, C. Duffalo, Intestinal microbiota, microbial translocation, and systemic
930 inflammation in chronic HIV infection. *Journal of Infectious Diseases* **211**, (2015).
931 23. C. L. Monaco *et al.*, Altered virome and bacterial microbiome in Human Immunodeficiency Virus-
932 associated Acquired Immunodeficiency Syndrome. *Cell Host & Microbe* **19**, 311-322 (2016).
933 24. F. Dossou-Yovo *et al.*, Metronidazole or cotrimoxazole therapy is associated with a decrease in
934 intestinal bioavailability of common antiretroviral drugs. *PLoS ONE* **9**, e89943 (2014).

25. I. Pandrea *et al.*, Antibiotic and anti-inflammatory therapy transiently reduces inflammation and hypercoagulation in acutely SIV-infected pigtailed macaques. *PLoS Pathogens* **12**, e1005384 (2016).
26. M. W. Ghilchik, A. S. Morris, D. S. Reeves, Immunosuppressive powers of the antibacterial agent trimethoprim. *Nature* **227**, 393-394 (1970).
27. G. Federico, M. Fantoni, F. Pallavicini, F. Ricci, A. Antinori, *In vivo* study in healthy volunteers on the effect of tetracycline and cotrimoxazole on chemiluminescence and granulocyte adhesion. *Quaderni Sclavo di diagnostica clinica e di laboratorio* **22**, 201-208 (1986).
28. R. Anderson, G. Grabow, R. Oosthuizen, A. Theron, A. J. Van Rensburg, Effects of sulfamethoxazole and trimethoprim on human neutrophil and lymphocyte functions *in vitro*: *in vivo* effects of co-trimoxazole. *Antimicrobial Agents & Chemotherapy* **17**, 322-326 (1980).
29. O. Pos, A. Stevenhagen, P. L. Meenhorst, F. P. Kroon, R. Van Furth, Impaired phagocytosis of *Staphylococcus aureus* by granulocytes and monocytes of AIDS patients. *Clinical & Experimental Immunology* **88**, 23-28 (1992).
30. P. M. Gaylarde, I. Sarkany, Suppression of thymidine uptake of human lymphocytes by co-trimoxazole. *British medical journal* **3**, 144-146 (1972).
31. N. M. Wolfish, N. Wassef, H. Gonzalez, C. Acharya, Immunologic parameters of children with urinary tract infection: effects of trimethoprim-sulfamethoxazole. *Canadian Medical Association journal* **112**, 76-79 (1975).
32. V. Dubar *et al.*, The penetration of co-trimoxazole into alveolar macrophages and its effect on inflammatory and immunoregulatory functions. *Journal of Antimicrobial Chemotherapy* **26**, 791-802 (1990).
33. M. Bwakura-Dangarembizi *et al.*, A randomized trial of prolonged co-trimoxazole in HIV-infected children in Africa. *New England Journal of Medicine* **370**, 41-53 (2014).
34. E. K. Gough *et al.*, The impact of antibiotics on growth in children in low and middle income countries: systematic review and meta-analysis of randomised controlled trials. *British medical journal* **348**, g2267 (2014).
35. A. Prendergast, A. S. Walker, V. Mulenga, C. Chintu, D. M. Gibb, Improved growth and anemia in HIV-infected African children taking cotrimoxazole prophylaxis. *Clinical infectious diseases : an official publication of the Infectious Diseases Society of America* **52**, 953-956 (2011).
36. A. J. Prendergast *et al.*, Stunting is characterized by chronic inflammation in Zimbabwean infants. *PLoS ONE* **9**, (2014).
37. S. Attia *et al.*, Mortality in children with complicated severe acute malnutrition is related to intestinal and systemic inflammation: an observational cohort study. *The American Journal of Clinical Nutrition*, (2016).
38. J. V. Giorgi, L. E. Hultin, J. A. McKeating, Shorter survival in advanced human immunodeficiency virus type 1 infection is more closely associated with T lymphocyte activation than with plasma virus burden or virus chemokine coreceptor usage. *Journal of Infectious Diseases* **179**, (1999).
39. Z. Liu *et al.*, Elevated CD38 antigen expression on CD8+ T cells is a stronger marker for the risk of chronic HIV disease progression to AIDS and death in the Multicenter AIDS Cohort Study than CD4+ cell count, soluble immune activation markers, or combinations of HLA-DR and CD38 expression. *Journal of Acquired Immune Deficiency Syndromes & Human Retrovirology* **16**, 83-92 (1997).
40. S. Tanaskovic, S. Fernandez, P. Price, S. Lee, M. A. French, CD31 (PECAM-1) is a marker of recent thymic emigrants among CD4+ T-cells, but not CD8+ T-cells or γδ T-cells, in HIV patients responding to ART. *Immunology & Cell Biology* **88**, 321 (2010).
41. C. P. Neff *et al.*, Fecal microbiota composition drives immune activation in HIV-infected individuals. *EBioMedicine* **30**, 192-202 (2018).
42. K. J. Marwa *et al.*, Resistance to cotrimoxazole and other antimicrobials among isolates from HIV/AIDS and non-HIV/AIDS patients at Bugando Medical Centre, Mwanza, Tanzania. *AIDS Research & Treatment* **2015**, 103874 (2015).
43. J. Mwansa, K. Mutela, I. Zulu, B. Amadi, P. Kelly, Antimicrobial sensitivity in Enterobacteria from AIDS patients, Zambia. *Emerging Infectious Diseases* **8**, 92-93 (2002).
44. K. M. Powis *et al.*, Cotrimoxazole prophylaxis was associated with enteric commensal bacterial resistance among HIV-exposed infants in a randomized controlled trial, Botswana. *Journal of the International AIDS Society* **20**, e25021-n/a (2017).
45. M. Scholz *et al.*, Strain-level microbial epidemiology and population genomics from shotgun metagenomics. *Nature methods* **13**, 435 (2016).

46. M. Choi *et al.*, Extracellular signal-regulated kinase inhibition by statins inhibits neutrophil activation by ANCA. *Kidney international* **63**, 96-106 (2003).
47. S. Dunzendorfer *et al.*, Mevalonate-dependent inhibition of transendothelial migration and chemotaxis of human peripheral blood neutrophils by pravastatin. *Circulation research* **81**, 963-969 (1997).
48. K. M. Harper, M. Mutasa, A. J. Prendergast, J. Humphrey, A. R. Manges, Environmental enteric dysfunction pathways and child stunting: A systematic review. *PLoS neglected tropical diseases* **12**, e0006205 (2018).
49. D. Lau *et al.*, Myeloperoxidase mediates neutrophil activation by association with CD11b/CD18 integrins. *Proceedings of the National Academy of Sciences* **102**, 431-436 (2005).
50. T. W. Chin, A. Vandenbroucke, I. W. Fong, Pharmacokinetics of trimethoprim-sulfamethoxazole in critically ill and non-critically ill AIDS patients. *Antimicrobial Agents and Chemotherapy* **39**, 28-33 (1995).
51. N. T. Funderburg *et al.*, Rosuvastatin reduces vascular inflammation and T cell and monocyte activation in HIV-infected subjects on antiretroviral therapy. *Journal of Acquired Immune Deficiency Syndromes* **68**, 396-404 (2015).
52. N. I. Paton, R. L. Goodall, D. T. Dunn, et al., Effects of hydroxychloroquine on immune activation and disease progression among HIV-infected patients not receiving antiretroviral therapy: A randomized controlled trial. *Journal of the American Medical Association* **308**, 353-361 (2012).
53. J. P. Routy *et al.*, Assessment of chloroquine as a modulator of immune activation to improve CD4 recovery in immune nonresponding HIV-infected patients receiving antiretroviral therapy. *HIV medicine* **16**, 48-56 (2015).
54. R. D. Moore, J. G. Bartlett, J. E. Gallant, Association between use of HMG CoA reductase inhibitors and mortality in HIV-infected patients. *PLoS ONE* **6**, e21843 (2011).
55. WHO, UNAIDS, Unicef, Global HIV/AIDS Epidemic update and health sector progress towards Universal Access. (2011).
56. I. Sereti *et al.*, Persistent, albeit reduced, chronic inflammation in persons starting antiretroviral therapy in acute HIV infection. *Clinical infectious diseases : an official publication of the Infectious Diseases Society of America* **64**, 124-131 (2017).
57. W. Jiang, M. M. Lederman, P. Hunt, Plasma levels of bacterial DNA correlate with immune activation and the magnitude of immune restoration in persons with antiretroviral-treated HIV infection. *Journal of Infectious Diseases* **199**, (2009).
58. A. R. Tenorio *et al.*, Soluble markers of inflammation and coagulation but not T-Cell activation predict non–AIDS-defining morbid events during suppressive antiretroviral treatment. *Journal of Infectious Diseases* **210**, 1248-1259 (2014).
59. M. D. Hazenberg *et al.*, Establishment of the CD4+ T-cell pool in healthy children and untreated children infected with HIV-1. *Blood* **104**, 3513-3519 (2004).
60. C. D. Doern, C.-A. D. Burnham, It's not easy being green: the Viridans Group Streptococci, with a focus on pediatric clinical manifestations. *Journal of Clinical Microbiology* **48**, 3829-3835 (2010).
61. B. Van den Bogert *et al.*, Comparative genomics analysis of Streptococcus isolates from the human small intestine reveals their adaptation to a highly dynamic ecosystem. *PLoS ONE* **8**, e83418 (2014).
62. G. Li *et al.*, Diversity of duodenal and rectal microbiota in biopsy tissues and luminal contents in healthy volunteers. *Journal of Microbiology & Biotechnology* **25**, 1136-1145 (2015).
63. P. Vonaesch *et al.*, Stunted childhood growth is associated with decompartmentalization of the gastrointestinal tract and overgrowth of oropharyngeal taxa. *Proceedings of the National Academy of Sciences* **115**, E8489-e8498 (2018).
64. A. J. Prendergast *et al.*, Stunting is characterized by chronic inflammation in Zimbabwean infants. *PLoS ONE* **9**, e86928 (2014).
65. B. van den Bogert, M. Meijerink, E. G. Zoetendal, J. M. Wells, M. Kleerebezem, Immunomodulatory properties of Streptococcus and Veillonella isolates from the human small intestine microbiota. *PLoS ONE* **9**, e114277 (2014).
66. R. C. Allen, J. T. Stephens, Myeloperoxidase selectively binds and selectively kills microbes. *Infection & Immunity* **79**, 474-485 (2011).
67. A. Abou-Eisha, A. Creus, R. Marcos, Genotoxic evaluation of the antimicrobial drug, trimethoprim, in cultured human lymphocytes. *Mutation research* **440**, 157-162 (1999).
68. A. M. Ortiz *et al.*, Experimental microbial dysbiosis does not promote disease progression in SIV-infected macaques. *Nature Medicine* **24**, 1313-1316 (2018).
69. S. Heuston, M. Begley, C. G. Gahan, C. Hill, Isoprenoid biosynthesis in bacterial pathogens. *Microbiology (Reading, England)* **158**, 1389-1401 (2012).

70. M. A. Elmore, R. H. Daniels, M. E. Hill, M. J. Finnen, Inhibition of neutrophil priming by inhibitors of farnesyl transferase. *Biochemical Society transactions* **25**, 253s (1997).
71. R. Terkeltaub, J. Solan, M. Barry, Jr., D. Santoro, G. M. Bokoch, Role of the mevalonate pathway of isoprenoid synthesis in IL-8 generation by activated monocytic cells. *Journal of leukocyte biology* **55**, 749-755 (1994).
72. E. Furrie *et al.*, Toll-like receptors-2, -3 and -4 expression patterns on human colon and their regulation by mucosal-associated bacteria. *Immunology* **115**, 565-574 (2005).
73. J. D. Keenan *et al.*, Azithromycin to reduce childhood mortality in Sub-Saharan Africa. *New England Journal of Medicine* **378**, 1583-1592 (2018).
74. A. Kekitiinwa *et al.*, Routine versus clinically driven laboratory monitoring and first-line antiretroviral therapy strategies in African children with HIV (ARROW): a 5-year open-label randomised factorial trial. *The Lancet* **381**, 1391-1403 (2013).
75. *Antiretroviral therapy for HIV infection in infants and children: towards universal access: Recommendations for a public health approach* (2006).
76. M. Bwakura-Dangarembizi *et al.*, Prevalence of lipodystrophy and metabolic abnormalities in HIV-infected African children after 3 years on first-line antiretroviral therapy. *Pediatric Infectious Diseases Journal* **34**, e23-31 (2015).
77. D. T. Truong *et al.*, MetaPhlAn2 for enhanced metagenomic taxonomic profiling. *Nature methods* **12**, 902-903 (2015).
78. S. Abubucker *et al.*, Metabolic reconstruction for metagenomic data and its application to the human microbiome. *PLoS Computational Biology* **8**, e1002358 (2012).
79. R. D. Finn *et al.*, Pfam: the protein families database. *Nucleic acids research* **42**, D222-230 (2014).
80. E. Z. Chen, H. Li, A two-part mixed-effects model for analyzing longitudinal microbiome compositional data. *Bioinformatics (Oxford, England)* **32**, 2611-2617 (2016).
81. X. Peng, G. Li, Z. Liu, Zero-inflated Beta regression for differential abundance analysis with metagenomics data. *Journal of Computational Biology*, (2015).
82. R. A. Rigby, D. M. Stasinopoulos, Generalized additive models for location, scale and shape. *Journal of the Royal Statistical Society: Series C (Applied Statistics)* **54**, 507-554 (2005).
83. Y. Benjamini, Y. Hochberg, Controlling the False Discovery Rate: a practical and powerful approach to multiple testing. *Journal of the Royal Statistical Society. Series B (Methodological)* **57**, 289-300 (1995).
84. P. Dixon, M. W. Palmer, VEGAN, a package of R functions for community ecology. *Journal of Vegetation Science* **14**, 927-930 (2003).
85. K. JD, J. McKean, Rfit: Rank-based estimation for linear models. *R Journal* **4**, 57-64 (2012).

ACKNOWLEDGEMENTS

We thank the participants, caregivers, and staff from all the centers participating in the ARROW trial and the *in vitro* cotrimoxazole treatment study. Antiretroviral drugs for the ARROW trial were donated and HIV viral load and genotyping assays were funded by ViiV Healthcare/GlaxoSmithKline. Cotrimoxazole for the ARROW trial was provided by national programs/Ministries for Health in Uganda and Zimbabwe. Margaret Govha and Sandra Rukobo undertook ELISA assays in Zimbabwe. Macklyn Kihembo and Lydia Nakiire undertook immunophenotyping at Uganda Virus Research Institute/Medical Research Centre, Entebbe and Joint Clinical Research Centre, Kampala, in Uganda, respectively. Hannah Poulsom provided supervision and assistance with ARROW assays. Anele Waters, Sarah Murphy and James Hand at the Grahame Hayton Unit, Royal London Hospital assisted with participant recruitment to the *in vitro* cotrimoxazole study. Aine McKnight hosted all containment level 3 laboratory work at QMUL.

FUNDING

This study was funded by the Wellcome Trust (grants 093768/Z/10/Z and 108065/Z/15/Z to AJP), with operating funds sub-contracted to ARM. CDB is funded by a Sir Henry Dale Fellowship from the Wellcome Trust and the Royal Society, UK (206225/Z/17/Z). EKG was funded by a Canadian Institutes of Health Research Postdoctoral Fellowship. The ARROW trial was jointly funded by the UK Medical Research Council (MRC) grant numbers G0300400 (AJP, VM, MB-D, AK, NK, DMG, ASW) and G1001190 (AJP, VM, MB-D, AK, NK, DMG, ASW) and the UK Department for International Development (DFID) under the

MRC/DFID Concordat agreement. It was also part of the EDCTP2 programme supported by the European Union. The MRC Clinical Trials Unit at UCL (AJS, MJS, DMG, ASW) is supported by funding from the MRC (MC_UU_12023/26). The funders and medication donors had no role in any aspect of the study design, data accrual, data analysis, writing of the manuscript, or the decision to submit the manuscript for publication.

AUTHOR CONTRIBUTIONS

CDB and EKG: conceptualized and implemented experimental plans for *in vitro* studies and fecal microbiome respectively, analyzed the data, prepared the figures and tables and lead manuscript preparation. AS and CB conducted biomarker assays at the University of Zimbabwe. GP implemented biomarker assays at Joint Clinical Research Centre, Kampala, Uganda. LT screened and recruited HIV-positive donors in the UK with oversight from JRD and CDB. CDB recruited HIV-negative donors in the UK; LB and YK assisted CDB with implementation of ELISA and Caco-2 assays respectively. NC provided initial Caco-2 stocks and guidance on their maintenance. DMG and ASW conceptualised and managed the ARROW trial; NK, AJP, ASW, DMG, MJS and AJS conceptualised and managed the associated immunology and virology sub-studies within ARROW. MBD, VM, JL and AK, recruited and conducted clinical follow-up of patients in the ARROW trial. CB processed and stored all stool samples in the ARROW trial. KM managed viral load assays and stool ELISA in Zimbabwe. MG and HMG assisted EKG with implementation and analysis of microbiome assays. CP provided support for HIV assays in the UK. TJE and ARM conducted PanPhlAn analysis of microbiome data. ASW conducted statistical analysis of ARROW biomarkers and prepared the associated figures. ASW and AJS conducted predictive models of the effect of

CRP and IL-6 on relative risk of adverse outcomes. AJP and ARM conceptualized the project, developed the overall research plan and had primary responsibility for the final content of the manuscript. All authors read and contributed to the manuscript, provided critical revisions, and approved its submission. None of the authors reported a conflict of interest related to the study. CDB and EKG contributed equally to this work. ARM and AJP also contributed equally to this work.

COMPETING INTERESTS

The authors declare no competing interests.

1145

1146 **FIGURES**

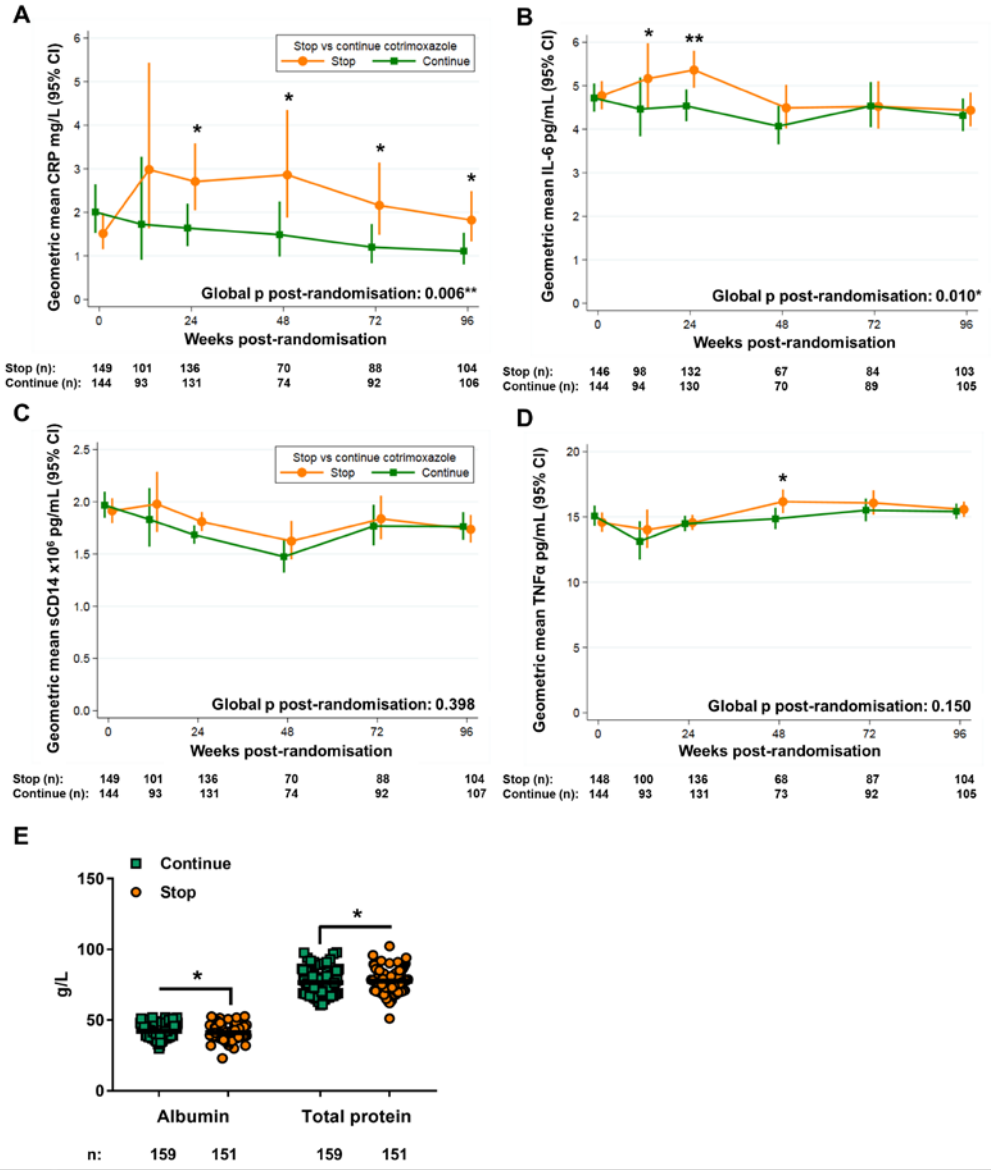

1147

1148 **Figure 1. Systemic inflammation is lower among HIV-positive children randomized to**
1149 **continue daily oral cotrimoxazole prophylaxis.** Biomarkers of systemic inflammation in
1150 longitudinal plasma samples from Zimbabwean and Ugandan children who had been
1151 receiving ART for ≥96 weeks with daily cotrimoxazole who were then randomized to stop
1152 (orange circles) or continue (green squares) cotrimoxazole. Geometric mean levels of (**A**)

1153

1154 CRP, (**B**) IL-6, (**C**) TNFα, and (**D**) sCD14 in plasma. Randomized groups were compared
1155 across all time-points using generalized estimating equations and at individual time-points
1156 using standard regression models (binomial distribution for viral load suppression, otherwise
1157 normal distribution for log-transformed values), all adjusted for centre and baseline
1158 biomarker levels (global p; **A**-**D**); *p<0.05, **p<0.01 ***p<0.001. (**E**) Serum levels of
1159 protein at week-48 post-randomization; horizontal bars indicate means. Comparisons between
1160 groups were made by Mann-Whitney U test; *p<0.05, **p<0.01 ***p<0.001.

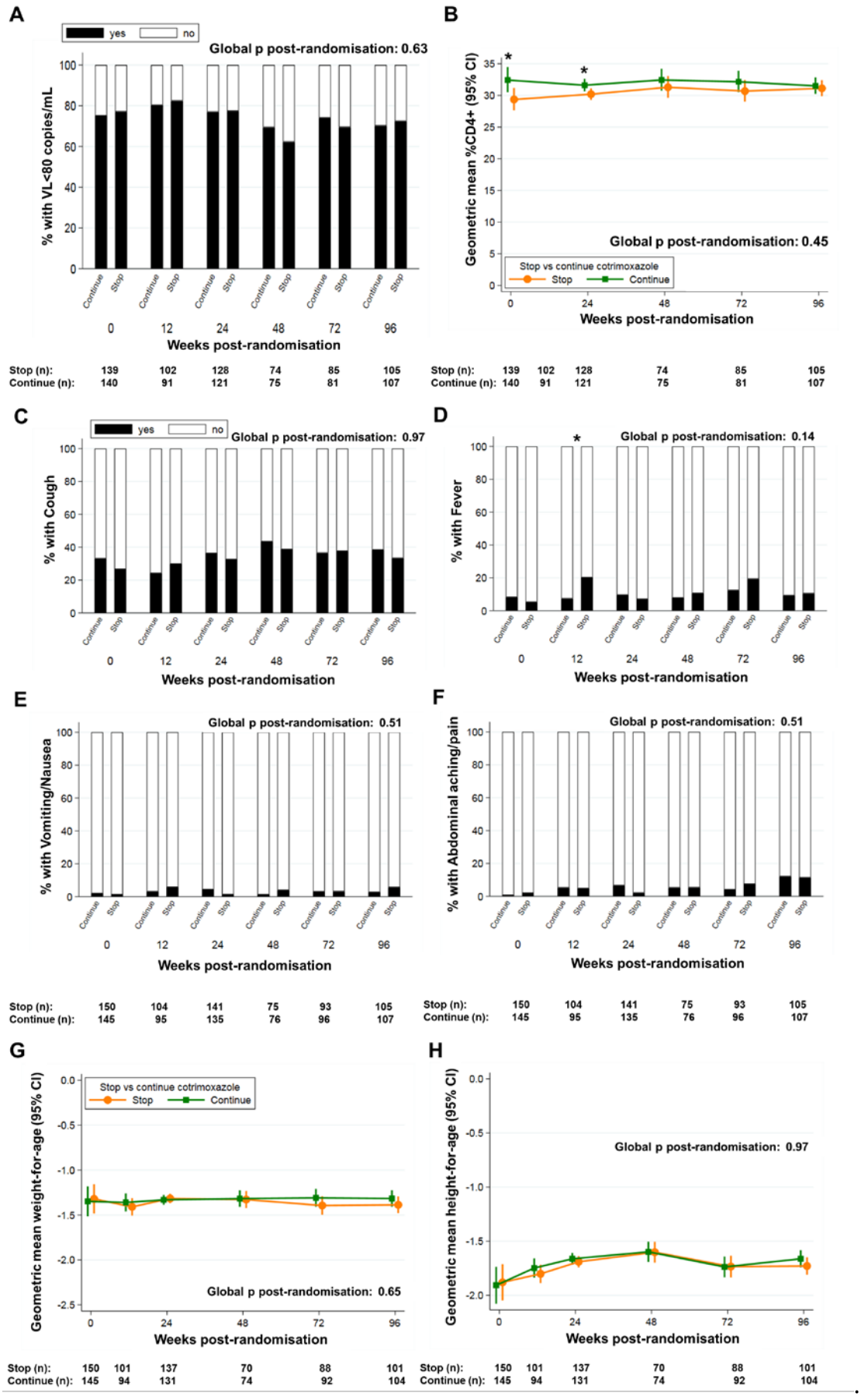
A
yes
no
Global p post-randomisation: 0.63
% with VL<80 copies/mL
Continue
Stop
0
12
24
48
72
96
Weeks post-randomisation
Stop (n): 139 102 128 74 85 105
Continue (n): 140 91 121 75 81 107
B
Geometric mean %CD4+ (95% CI)
Global p post-randomisation: 0.45
Stop vs continue cotrimoxazole
Stop
Continue
Weeks post-randomisation
Stop (n): 139 102 128 74 85 105
Continue (n): 140 91 121 75 81 107
C
yes
no
Global p post-randomisation: 0.97
% with Cough
Weeks post-randomisation
D
Global p post-randomisation: 0.14
% with Fever
Weeks post-randomisation
E
Global p post-randomisation: 0.51
% with Vomiting/Nausea
Weeks post-randomisation
Stop (n): 150 104 141 75 93 105
Continue (n): 145 95 135 76 96 107
F
Global p post-randomisation: 0.51
% with Abdominal aching/pain
Weeks post-randomisation
Stop (n): 150 104 141 75 93 105
Continue (n): 145 95 135 76 96 107
G
Stop vs continue cotrimoxazole
Stop
Continue
Geometric mean weight-for-age (95% CI)
Global p post-randomisation: 0.65
Weeks post-randomisation
Stop (n): 150 101 137 70 88 101
Continue (n): 145 94 131 74 92 104
H
Geometric mean height-for-age (95% CI)
Global p post-randomisation: 0.97
Weeks post-randomisation
Stop (n): 150 101 137 70 88 101
Continue (n): 145 94 131 74 92 104

1161

1162

1163 **Figure 2. Cotrimoxazole effects on systemic inflammation are not solely due to**
1164 **differences in HIV disease progression, symptomatic infections or nutritional status.** (**A**)
1165 Percentage of children with HIV suppression (viral load <80 copies/mL), (**B**) geometric mean
1166 percentage CD4+ T-cells, proportions of children with caregiver-reported (**C**) cough, (**D**)
1167 fever, (**E**) vomiting/nausea and (**F**) abdominal pain, geometric mean (**G**) weight-for-age and
1168 (**H**) height-for-age Z scores were quantified longitudinally in children randomized to
1169 continue versus stop cotrimoxazole prophylaxis. The number of samples per randomized
1170 group is shown under each graph. Longitudinal data were compared between randomized
1171 groups by generalized estimating equations across all time-points (global p) and at individual
1172 time-points using standard regression models (binomial distribution for viral load
1173 suppression, otherwise normal distribution for log transformed values) adjusted for
1174 recruitment centre; *p<0.05, **p<0.01 ***p<0.001.

1175

1176

1177

1178

1179

1180

1181

1182

1183

1184

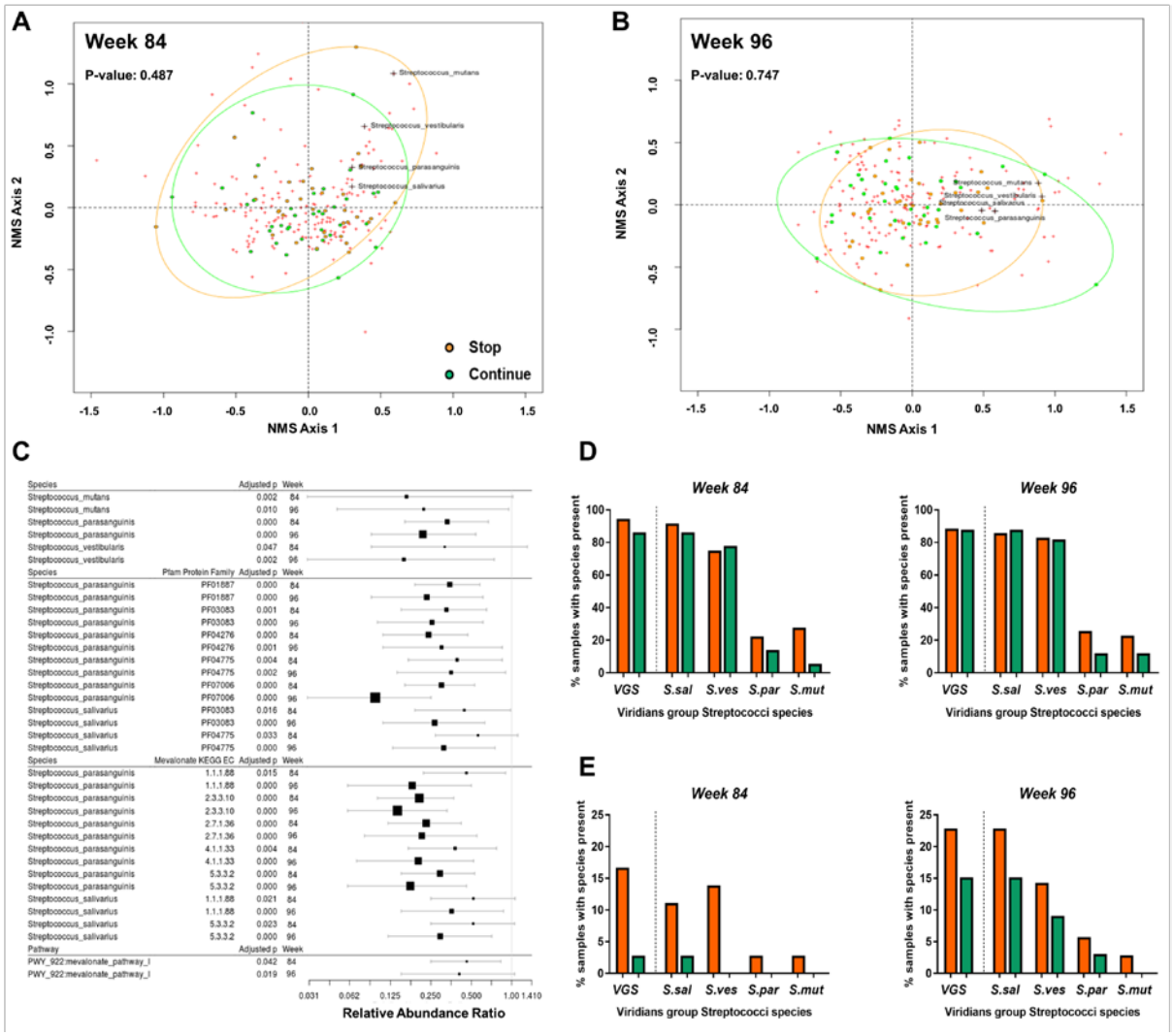

1185

1186 **Figure 3. Continuation of cotrimoxazole specifically suppresses the abundance and**
1187 **function of viridians group Streptococci in randomized fecal samples from HIV-positive**
1188 **children.** Non-metric multidimensional scaling (NMDS) plots of the Bray–Curtis dissimilarity
1189 index of species-level fecal microbiomes from 72 HIV-positive Zimbabwean children
1190 randomized to stop (orange) versus continue (green) cotrimoxazole prophylaxis in the
1191 ARROW trial at (**A**) week-84 and (**B**) week-96 post-randomization. Each dot represents the
1192 global fecal bacterial species community composition of each child and the distance between
1193 them indicates their relative similarity/dissimilarity. Red crosses indicate distribution of
1194 individual bacterial species within the cohort irrespective of randomized group; VGS species

that consistently differed according to cotrimoxazole treatment are labelled. Results of permutation tests for global differences between randomized cotrimoxazole treatment groups are indicated. (**C**) Effect size plots showing relative abundance ratios (± 95% confidence interval) for all *Streptococcus* spp. and the protein families (Pfam), metabolic pathways and mevalonate pathway-associated genes with identity to *Streptococcus* spp. that significantly differed in abundance between children who continued versus those who stopped cotrimoxazole at both week-84 and week-96 post-randomization in zero-inflated beta regression analysis after FDR adjustment for multiple hypothesis testing. The identities of bacterial species for each Pfam and mevalonate enzyme were established using HUMANn2 with default settings against the UniRef90 database. Relative abundance ratio less than 1.0 indicates a decrease in relative abundance in children randomized to continue versus stop cotrimoxazole. The size of the squares is inversely proportional to the magnitude of the FDR-adjusted p values. The vertical grey line indicates the null value. Effect size plots for full lists of differentially abundant species and Pfam, are available in **fig. S2** and **S3**. Percentage of samples that were positive for any of the four VGS or individual species according to (**D**) MetaPhlAn and (**E**) PanPhlAn analysis at week-84 (Continue n=36 and Stop n=36) and week-96 (Continue n=33 and Stop n=35).

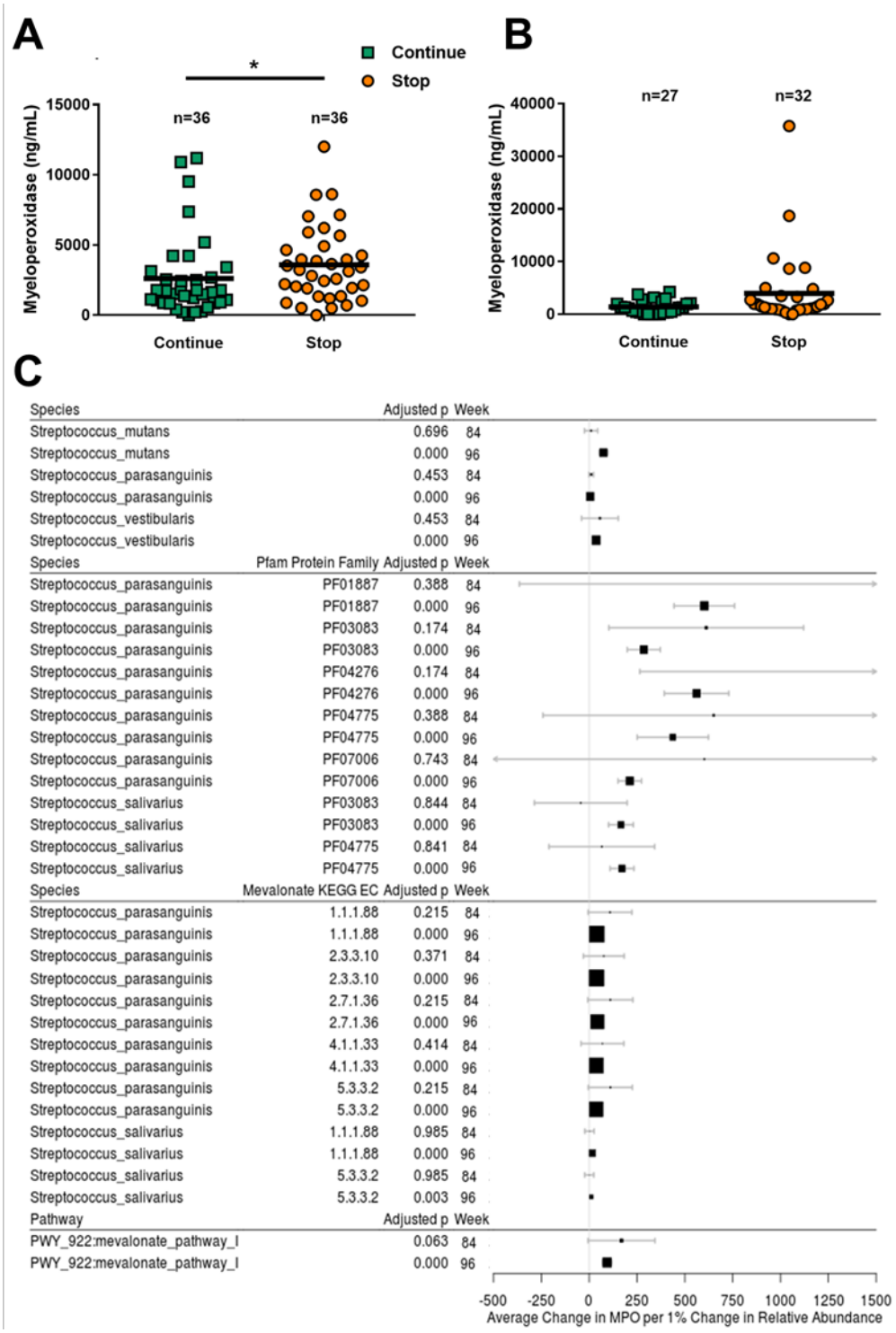

Figure 4. Intestinal inflammation is positively associated with fecal viridians group Streptococci that are suppressed by continuation of cotrimoxazole prophylaxis among HIV-positive children. Myeloperoxidase levels assayed at (**A**) week-84 and (**B**) week-96 in

fecal samples from HIV-positive Zimbabwean children randomized to stop versus continue cotrimoxazole prophylaxis. Randomized groups were compared by Mann-Whitney U test; *p<0.05, horizontal lines indicate the median value. (**C**) Effect size plots showing the average change in myeloperoxidase per 1% change in relative abundance (± 95% confidence interval) for all *Streptococcus* spp., and their protein families (Pfam), metabolic pathways and mevalonate pathway-associated genes that significantly differed in abundance between children who continued versus those who stopped cotrimoxazole at both week-84 and week-96 post-randomization in zero-inflated beta regression analysis after FDR adjustment for multiple hypothesis testing (**Fig. 3C**). Identities of bacterial species for each Pfam and mevalonate enzyme were established using HUMANn2 with default settings against the UniRef90 database. The size of the squares is inversely proportional to the magnitude of the FDR-adjusted p values. The vertical grey line indicates the null value. Effect size plots for full lists of differentially abundant species and Pfam are available in **fig. S5** and **S6**.

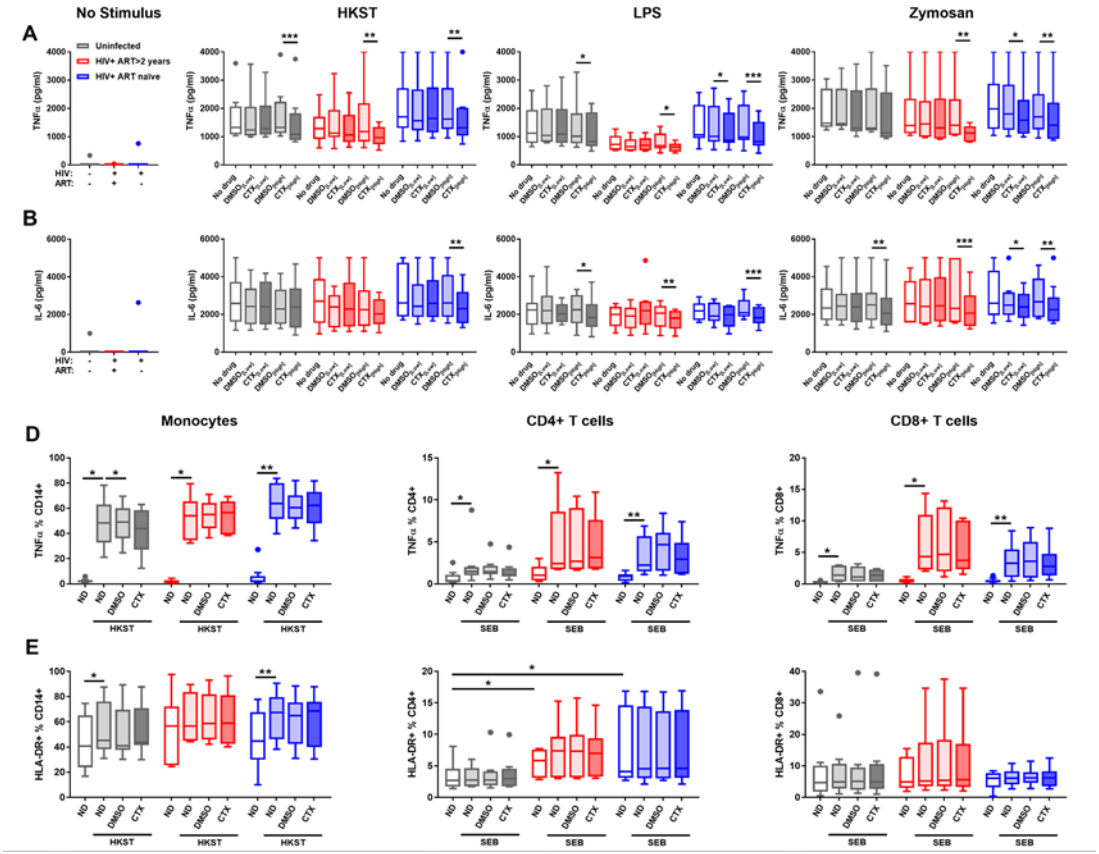

Figure 5. Cotrimoxazole inhibits *in vitro* pro-inflammatory cytokine responses to bacterial and fungal antigens. Tukey boxplots of (**A**) TNFα and (**B**) IL-6 levels in supernatants from whole blood cultures without antigen (No stimulus; far left), with 10^8 cells/mL heat-killed *Salmonella typhimurium* (HKST; centre left), 5 EU/mL lipopolysaccharide (LPS; centre right); or 5 μg/mL zymosan (far right). Cultures were treated with low-dose ($CTX_{[Low]}$: 2 μg/mL trimethoprim and 50 μg/mL sulfamethoxazole), high-dose cotrimoxazole ($CTX_{[High]}$: 8 μg/mL trimethoprim and 200 μg/mL sulfamethoxazole) or volume-matched diluent controls ($DMSO_{[Low]}$ or $DMSO_{[High]}$). Proportions of monocytes (left), CD4+ (centre) and CD8+ T-cells producing (**C**) TNFα and expressing (**D**) HLA-DR after 6h PBMC culture. Blood samples from HIV-negative adults are in grey (n=8); HIV-positive ART-treated adults are in red (n=6); and HIV-positive ART-naïve adults are in blue

1245

1246](n=10). Cytokine levels in cotrimoxazole-treated cultures are indicated by darker shading.

1247 Drug treatments were compared within groups by Freidman tests with post-hoc Dunn's tests;

1248 *p<0.05, **p<0.01, ***p<0.001.

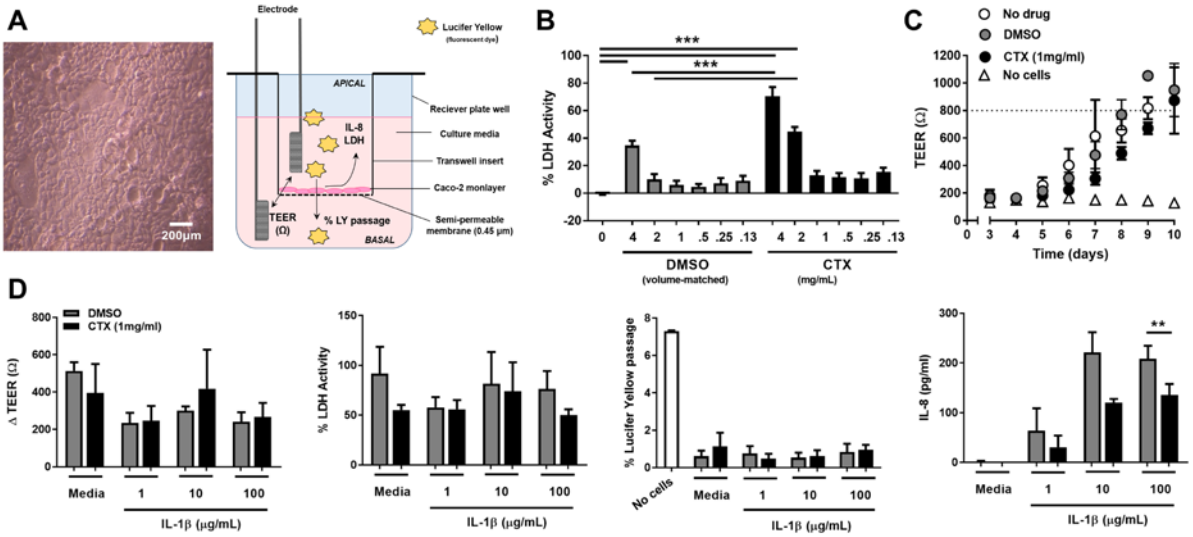

Figure 6. Long-term cotrimoxazole treatment reduces *in vitro* IL-8 production by gut epithelial cell monolayers under inflammatory conditions. (**A**) Light microscopy of confluent Caco-2 monolayer (200 µm scale bar; left) and a diagram of the transwell culture model (right). (**B**) Percentage lactose dehydrogenase activity relative to lysed cells (% LDH) of Caco-2 monolayers cultured for 24h with titrated concentrations of cotrimoxazole (CTX; black bars) or DMSO control (grey bars); % LDH was compared to untreated controls and between volume-matched pairs of cotrimoxazole and DMSO by Tukey's test adjusted for multiple comparisons; ***p<0.001. (**C**) Daily trans-epithelial resistance (TEER) measurements of transwell Caco-2 cultures with no drug (white circles), 1 mg/mL cotrimoxazole (black circles) or volume-matched DMSO control (grey circles) present throughout growth relative to transwells without Caco-2 (no cells; white triangles); mean ± SEM, n=3 separate experiments. Dotted line indicates the mean 800Ω TEER/plate threshold for stimulating cultures. (**D**) Caco-2 transwell cultures that had been treated with 1 mg/mL CTX or DMSO since seeding were incubated for 24h with media alone (no stimulus) or IL-1β at 1 µg/mL, 10 µg/mL or 100 µg/mL for 24h; mean ± SEM, n=3 separate experiments. For each experiment, graphs indicate the change in TEER from pre- to 24h post-treatment (Δ

TEER; far left), % LDH (centre left), % apical-to-basal passage of Lucifer Yellow dye relative to transwells without Caco-2 cells (centre right), and IL-8 concentration in apical supernatants (far right). Comparisons between cotrimoxazole- and DMSO-treated cultures were made by 2-tailed t-tests; *p<0.05, **p<0.01

1273 **SUPPLEMENTARY MATERIALS**

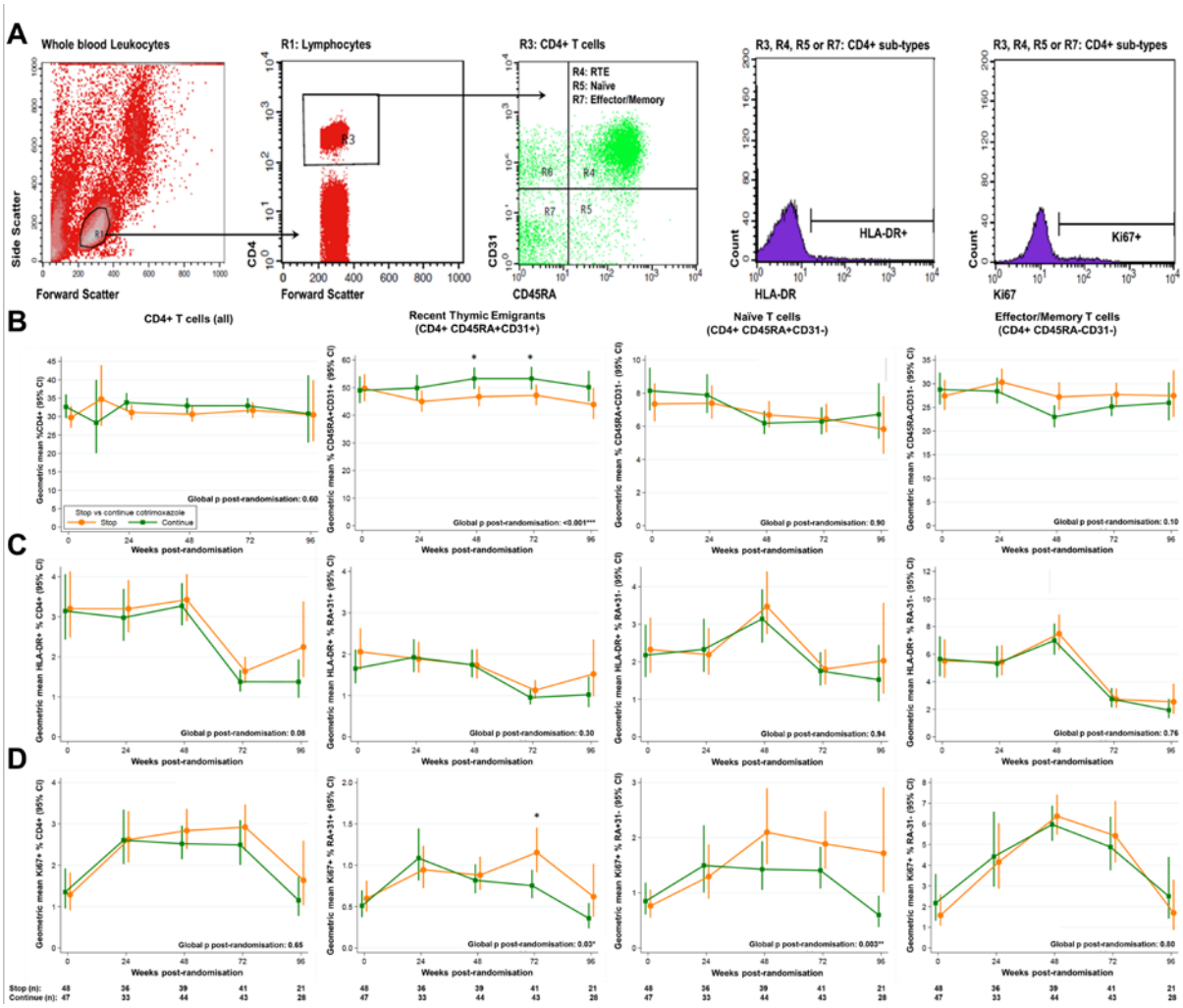

1274

1275

1276 **figure S1. Cotrimoxazole alters circulating CD4+ T-cell phenotype in HIV infection.** (**A**)
1277 Representative gating of flow cytometry data from uncultured blood leukocytes from HIV-
1278 positive ART-treated children randomized to stop (orange circles) versus continue (green
1279 squares) cotrimoxazole prophylaxis. Lymphocytes (R1) were gated on CD4 expression (R3)
1280 and sub-divided according to CD31 and CD45RA expression into: recent thymic emigrant-
1281 like (RTE; CD45RA+ CD31+; R4), naïve (CD45RA+ CD31-; R5) or effector-memory

(CD45RA-CD31-; R7) CD4+ T-cells. Graphs show the proportions of CD4+ T-cell subsets (**B**) and the proportion of each subset expressing the surface activation marker HLA-DR (**C**) or the intracellular proliferation marker Ki67 (**D**). Numbers of participants at each time-point are indicated below the graphs. Statistical comparisons between randomized groups were made using generalized estimating equations across all time-points (global p) and at individual time-points using standard regression models (normal distribution for log transformed values), all adjusted for centre and baseline percentages; *p<0.05, **p<0.01 ***p<0.001

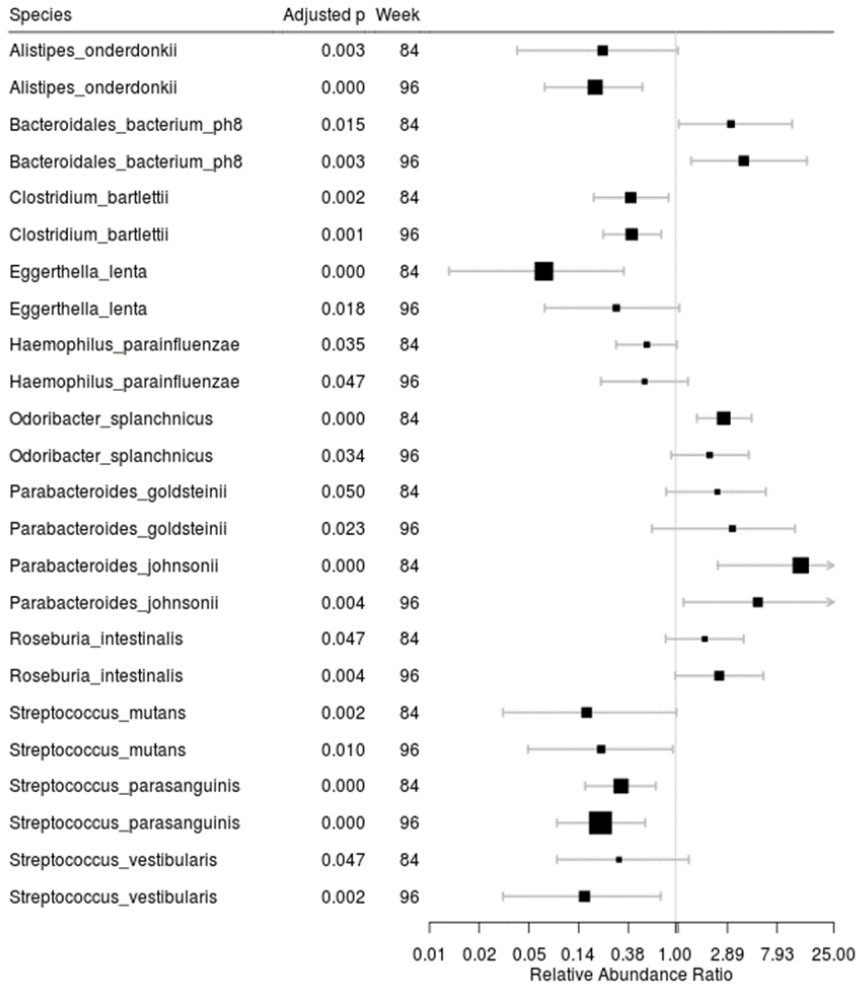

figure S2. Fecal bacterial species that differ between HIV-positive ART-treated Zimbabwean children randomized to continue versus stop cotrimoxazole prophylaxis. Effect size plots (relative abundance ratios ± 95% confidence interval) of bacterial species that had a consistent statistically significant difference in relative abundance at both week-84 and week-96 post-randomization to continue (n=36) versus stop (n=36) cotrimoxazole after FDR adjustment for multiple hypothesis testing (adjusted p<0.05). Relative abundance ratio less than 1.0 indicates a decrease in relative abundance in children randomized to continue versus stop cotrimoxazole. The size of the squares is inversely proportional to the magnitude of the FDR-adjusted p values. Vertical grey line indicates the null value. Comparison between randomized groups was made by zero-inflated beta regression.

1313

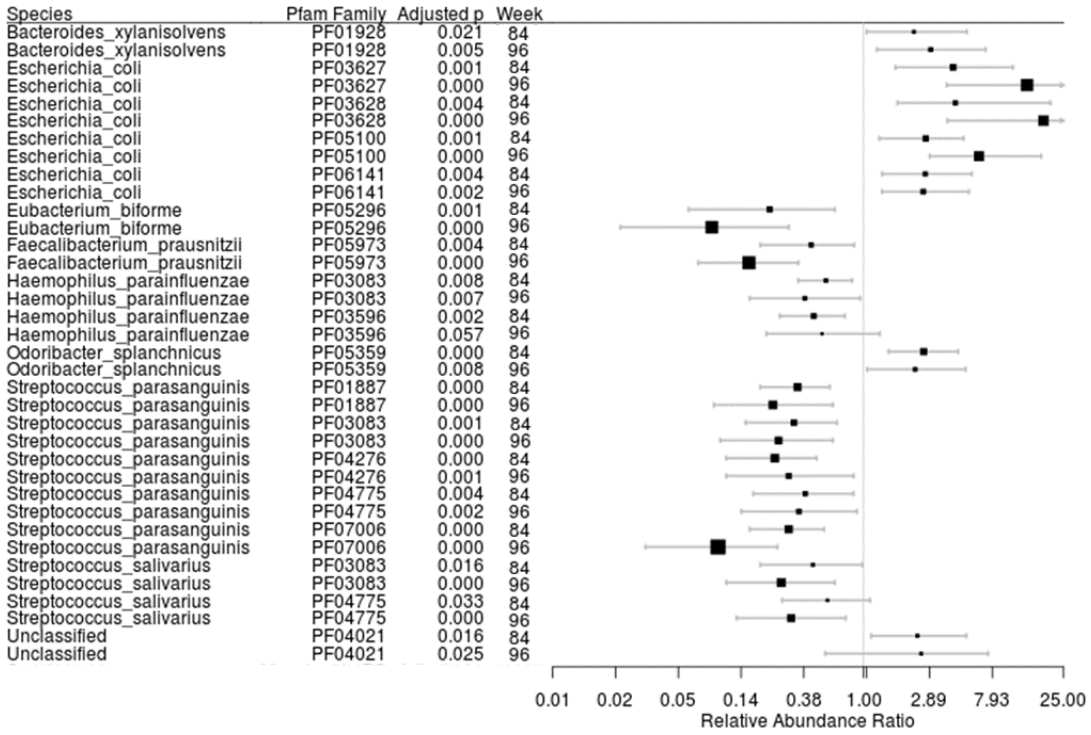

1314

1315 **figure S3. Protein families that differ in fecal samples between HIV-positive ART-**
1316 **treated Zimbabwean children randomized to continue versus stop cotrimoxazole**
1317 **prophylaxis.** Effect size plots (relative abundance ratios ± 95% confidence interval) of
1318 protein families (Pfam) that had a consistent statistically significant difference in relative
1319 abundance at both week-84 and week-96 post-randomization to continue (n=36) versus stop
1320 (n=36) cotrimoxazole after FDR adjustment for multiple hypothesis testing (adjusted
1321 $p<0.05$). Identities of bacterial species for each Pfam were established using HUMANn2 with
1322 default settings against the UniRef90 database. Relative abundance ratio less than 1.0
1323 indicates a decrease in relative abundance in children randomized to continue versus stop
1324 cotrimoxazole. The size of the squares is inversely proportional to the magnitude of the FDR-
1325 adjusted p values. Vertical grey line indicates the null value. Comparison between
1326 randomized groups was made by zero-inflated beta regression.

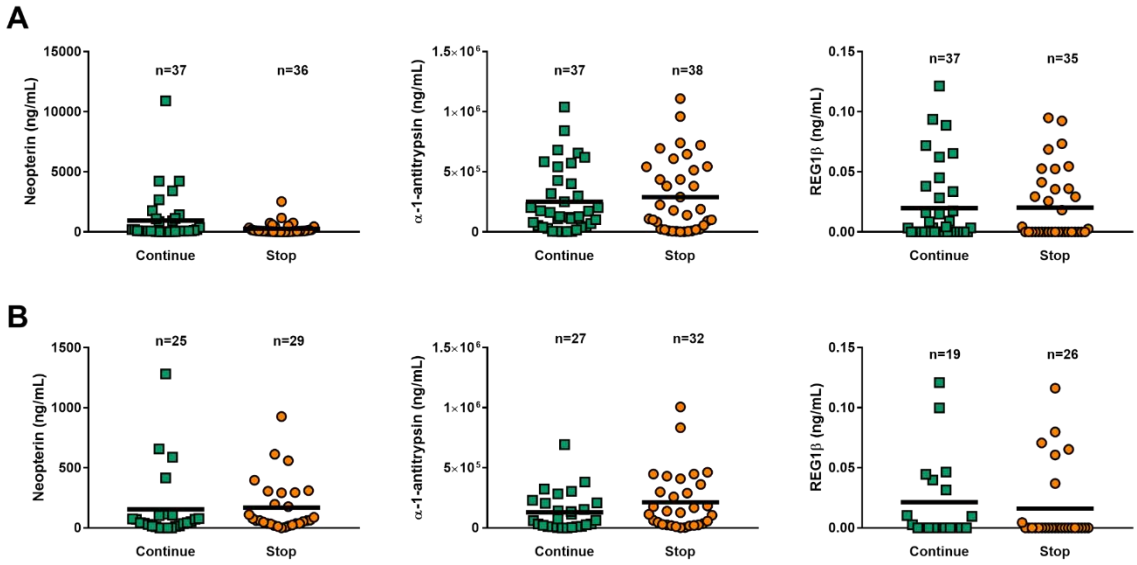

figure S4. Fecal biomarkers of enteropathy that were unaffected by continuing versus stopping cotrimoxazole prophylaxis. Concentrations of the enteropathy biomarkers neopterin, α-1-antitrypsin and regenerating family member 1 beta (REG1β) in fecal samples collected from HIV-positive ART-treated Zimbabwean children randomized to stop (orange circles) or continue (green squares) cotrimoxazole prophylaxis at (**A**) week-84 and (**B**) week-96 post-randomization within the ARROW trial. Comparisons were made between randomized groups by Mann-Whitney U test; $p>0.05$.

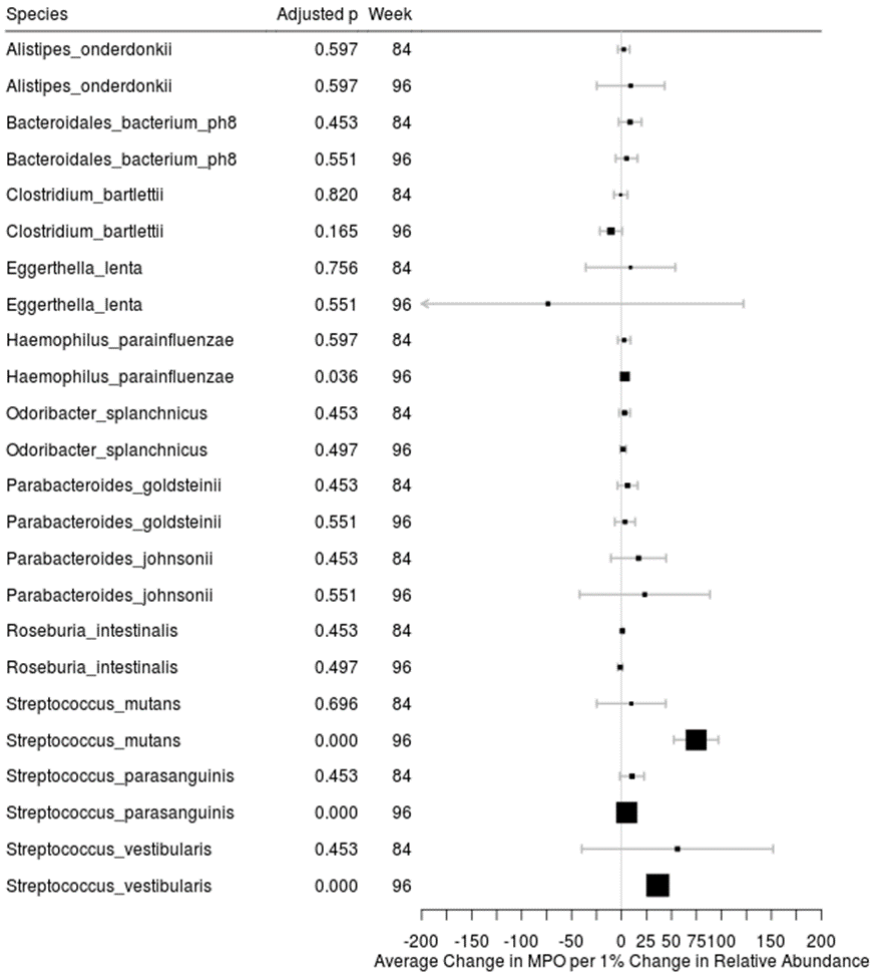

figure S5. Associations between all fecal bacterial species that differed between HIV-positive children randomized to continue versus stop cotrimoxazole prophylaxis and fecal levels of myeloperoxidase. Effect size plots showing the average change in fecal myeloperoxidase per 1% change in relative abundance (± 95% confidence interval) for all bacterial species that significantly differed in abundance between fecal samples from children randomized to continue versus stop cotrimoxazole at both week-84 and week-96 post-randomization in zero-inflated beta regression analysis after FDR adjustment for multiple hypothesis testing. The size of the squares is inversely proportional to the magnitude of the FDR-adjusted p values. The vertical grey line indicates the null value. **Fig. 4C** presents a condensed version of this analysis for *Streptococcal* spp.

1346

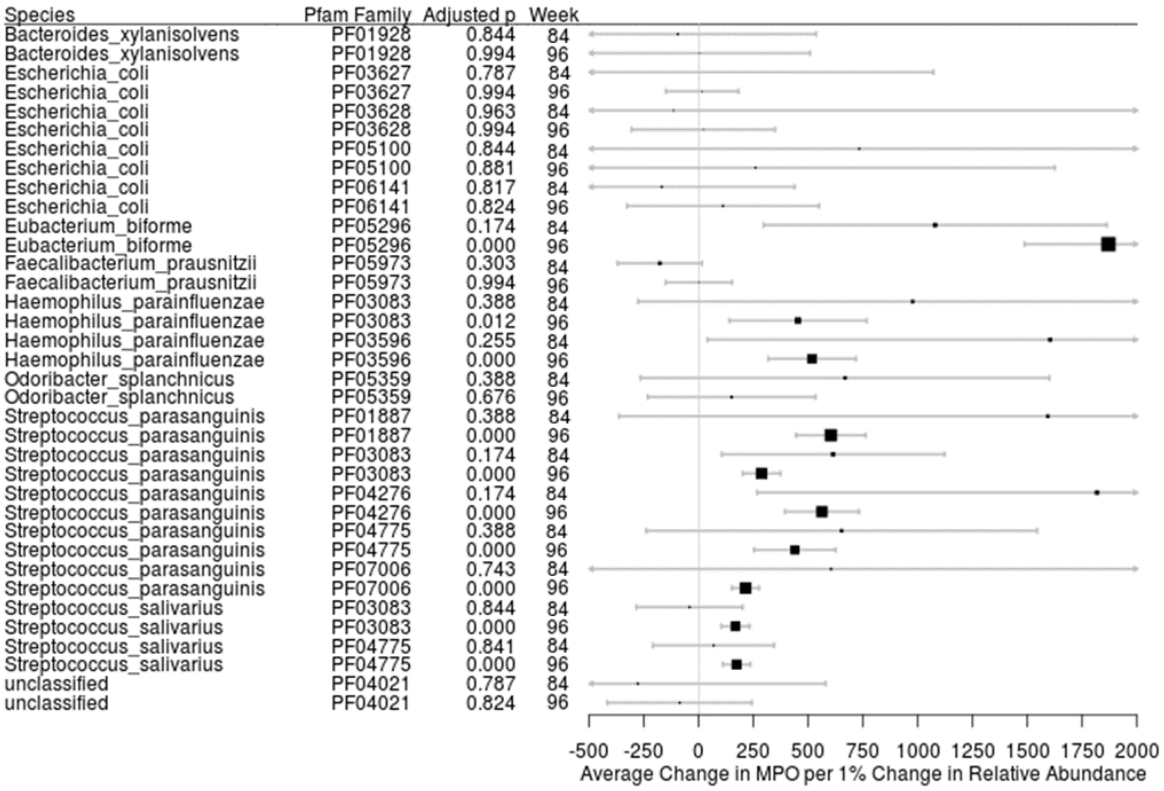

1347

1348 **figure S6. Associations between all fecal Pfam that differed between HIV-positive**
1349 **children randomized to continue versus stop cotrimoxazole prophylaxis and fecal levels**
1350 **of myeloperoxidase.** Effect size plots showing the average change in fecal myeloperoxidase
1351 per 1% change in relative abundance (± 95% confidence interval) for all Pfam that
1352 significantly differed in abundance between fecal samples children randomized to continue
1353 versus stop cotrimoxazole at both week-84 and week-96 post-randomization in zero-inflated
1354 beta regression analysis after FDR adjustment for multiple hypothesis testing. Identities of
1355 bacterial species for each Pfam were established using HUMANn2 with default settings
1356 against the UniRef90 database. The size of the squares is inversely proportional to the
1357 magnitude of the FDR-adjusted p values. The vertical grey line indicates the null value. **Fig.**
1358 **4C** presents a condensed version of this analysis for Pfam with identify to *Streptococcal* spp.

1359

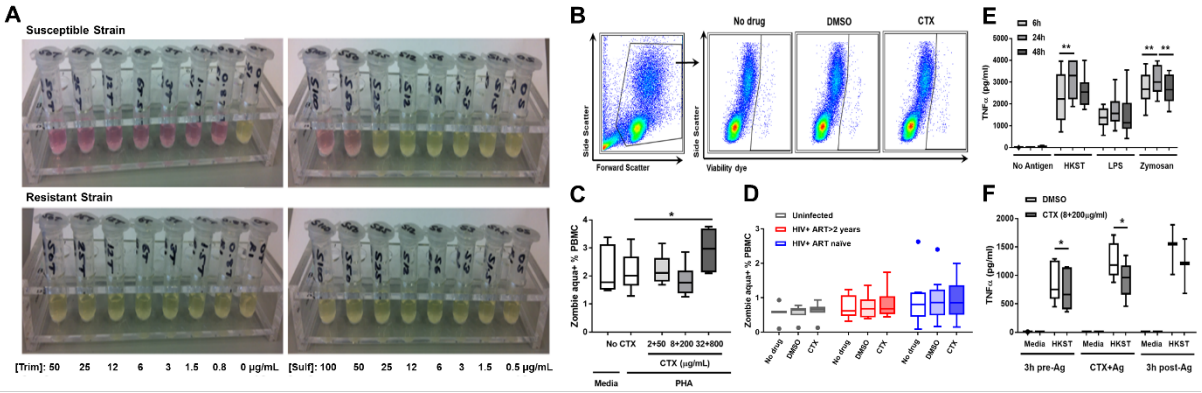

1361

1362 **figure S7. Optimization of *in vitro* blood leukocyte activation and cotrimoxazole**

1363 **treatment conditions.** (**A**) Photographs of 24h cultures of cotrimoxazole-susceptible (isolate

1364 ID: 15A076507S; top) and cotrimoxazole-resistant (isolate ID: 15A076598R; bottom)

1365 bacterial isolates from human urinary tract infections treated with titrated concentrations of

1366 trimethoprim (Trim, left) and sulfamethoxazole (Sulf, right) prepared in DMSO diluent;

1367 representative of 2 experimental repeats. Pink transparent media indicates an absence of

1368 bacterial growth, confirming that laboratory preparations of cotrimoxazole have antibiotic

1369 activity at minimum concentrations of 0.8 µg/mL trimethoprim and 50 µg/mL

1370 sulfamethoxazole. A yellow opaque appearance indicates bacterial growth, which, as

1371 expected, is not inhibited by co-culture of trimethoprim or sulfamethoxazole with resistant

1372 bacteria. (**B**) Flow cytometry gating strategy showing Zombie aqua cell viability staining

1373 (Biolegend; positive staining identifies dead cells) of unstimulated PBMC cultured for 6h

1374 without drug treatment, with cotrimoxazole (CTX: 8 µg/mL trimethoprim and 200 µg/mL

1375 sulfamethoxazole) or volume-matched DMSO control; representative of 24 samples. (**C**)

1376 Tukey boxplots showing median proportions of dead (Zombie aqua+) PBMC after 24h

1377 culture without antigen or with 1 µg/mL of mitogen (PHA) with titrated concentrations of

1378 cotrimoxazole. Cell death significantly increased at concentrations of 32µg/mL trimethoprim

1379

and 800µg/mL sulfamethoxazole, therefore subsequent *in vitro* doses were maintained below this threshold. Freidman's test with post-hoc uncorrected Dunn's; n=6, *p<0.05. (**D**) Tukey boxplots showing median proportions of dead (Zombie aqua+) cells in unstimulated 6h PBMC from HIV-negative (n=8, grey), HIV-positive ART-treated (n=8, red) and HIV-positive ART-naïve (n=10, blue) adults cultured for 6h without drug (ND) or with CTX at 8 µg/mL trimethoprim and 200 µg/mL sulfamethoxazole or volume-matched DMSO. None of the drug treatments affected cell viability relative to untreated cultures. (**E**) Tukey boxplots showing median TNFα concentrations in whole blood culture supernatants after 6, 24 or 48h culture with bacterial and fungal TLR ligands; Kruskall-Wallis with post-hoc uncorrected Dunn's test; n=6, **p<0.01. (**F**) Tukey boxplots showing median TNFα concentrations in whole blood culture supernatants after 24h culture with HKST and addition of CTX (8+200 µg/mL) for 3h before (3h pre-Ag), at the same time as (CTX+Ag) or 3h after (3h-post Ag) addition of HKST; Mann-Whitney U test; n=6, *p<0.05. 24h culture with TLR ligands and simultaneous cotrimoxazole treatment were chosen for subsequent experiments.

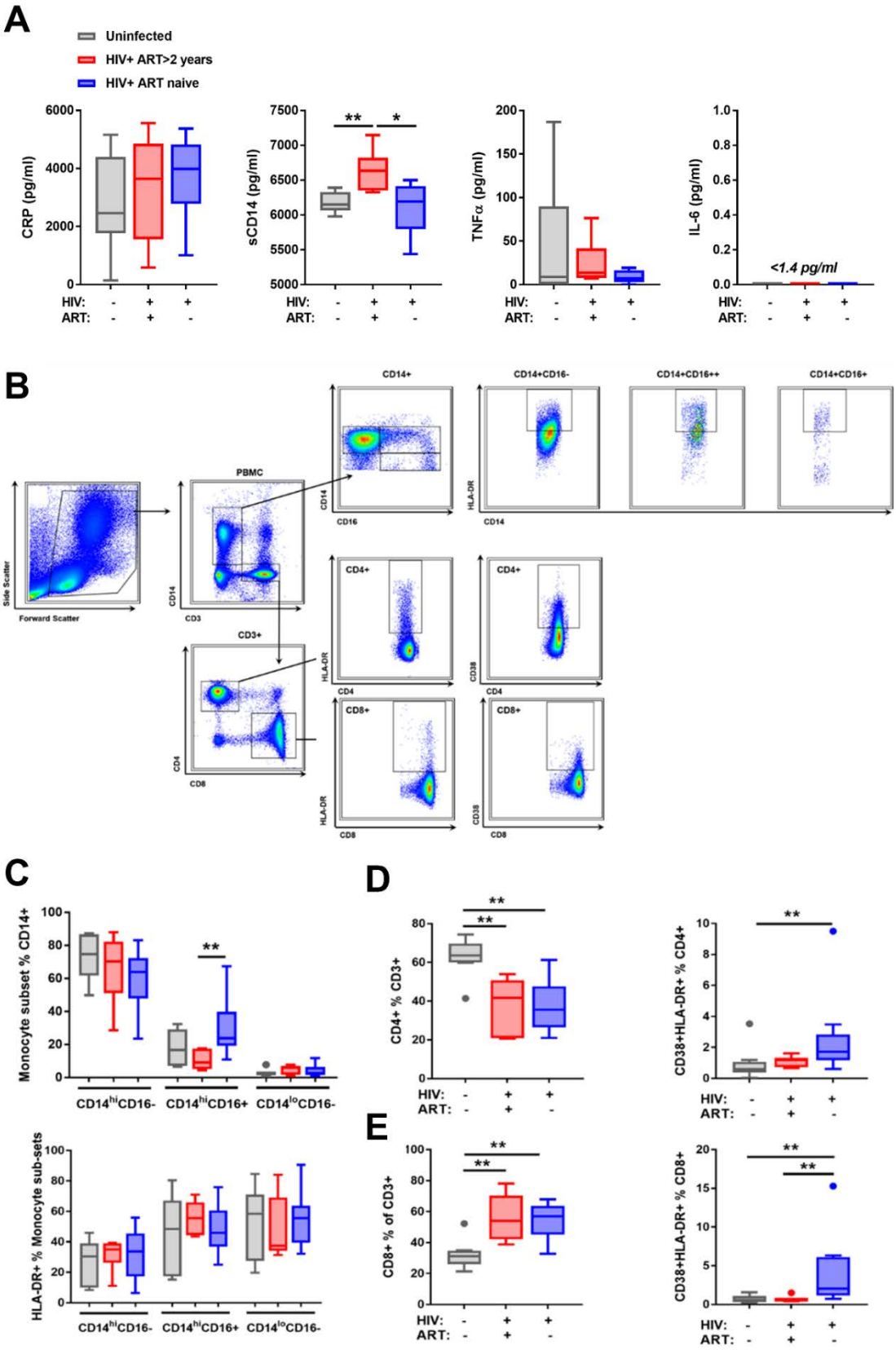
A
Uninfected
HIV+ ART>2 years
HIV+ ART naive
CRP (pg/ml)
sCD14 (pg/ml)
TNFα (pg/ml)
IL-6 (pg/ml)
<1.4 pg/ml
HIV:
ART:
B
PBMC
CD14+
CD14+CD16-
CD14+CD16++
CD14+CD16+
CD3+
CD4+
CD8+
C
Monocyte subset % CD14+
CD14hiCD16-
CD14hiCD16+
CD14loCD16-
HLA-DR+ % Monocyte sub-sets
D
CD4+ % CD3+
CD38+HLA-DR+ % CD4+
E
CD8+ % of CD3+
CD38+HLA-DR+ % CD8+

1397

1399 **figure S8. HIV-positive adults have greater systemic inflammation, monocyte and T-cell**
1400 **activation than HIV-negative adults.** Background inflammation and circulating immune
1401 cell activation was assessed in blood samples from HIV-negative (grey; n=8), HIV-positive
1402 ART-treated (red; n=6) and HIV-positive ART-naïve adults (blue; n=10) recruited in the UK
1403 (**A**) Levels of systemic inflammatory mediators in plasma samples. Levels of IL-6 were
1404 below the ELISA limit of detection in all three groups (<1.4 pg/mL). Statistical comparisons
1405 between groups were made using Kruskall-Wallis test with post-hoc pair-wise Dunn's test;
1406 *p<0.05, **p<0.01. (**B**) Representative flow cytometry gating strategy for monocyte and T-
1407 cell phenotyping in freshly isolated PBMC; representative of 24 samples. (**C**) Monocyte
1408 activation phenotype: proportions of monocyte sub-types segregated according to CD14 and
1409 CD16 expression (classical $CD14^{hi}CD16^{-}$; intermediate $CD14^{hi}CD16^{+}$; and non-classical
1410 $CD14^{lo}CD16^{+}$; above), and HLA-DR expression by monocyte sub-types (below). Proportions
1411 of (**D**) CD4+ and (**E**) CD8+ T-cells within the CD3+ T-cell pool (left) and proportions of T-
1412 cells co-expressing HLA-DR and CD38 markers associated with activation. Statistical
1413 comparisons between groups were made using Kruskall-Wallis test with post-hoc pair-wise
1414 Dunn's test; *p<0.05, **p<0.01.

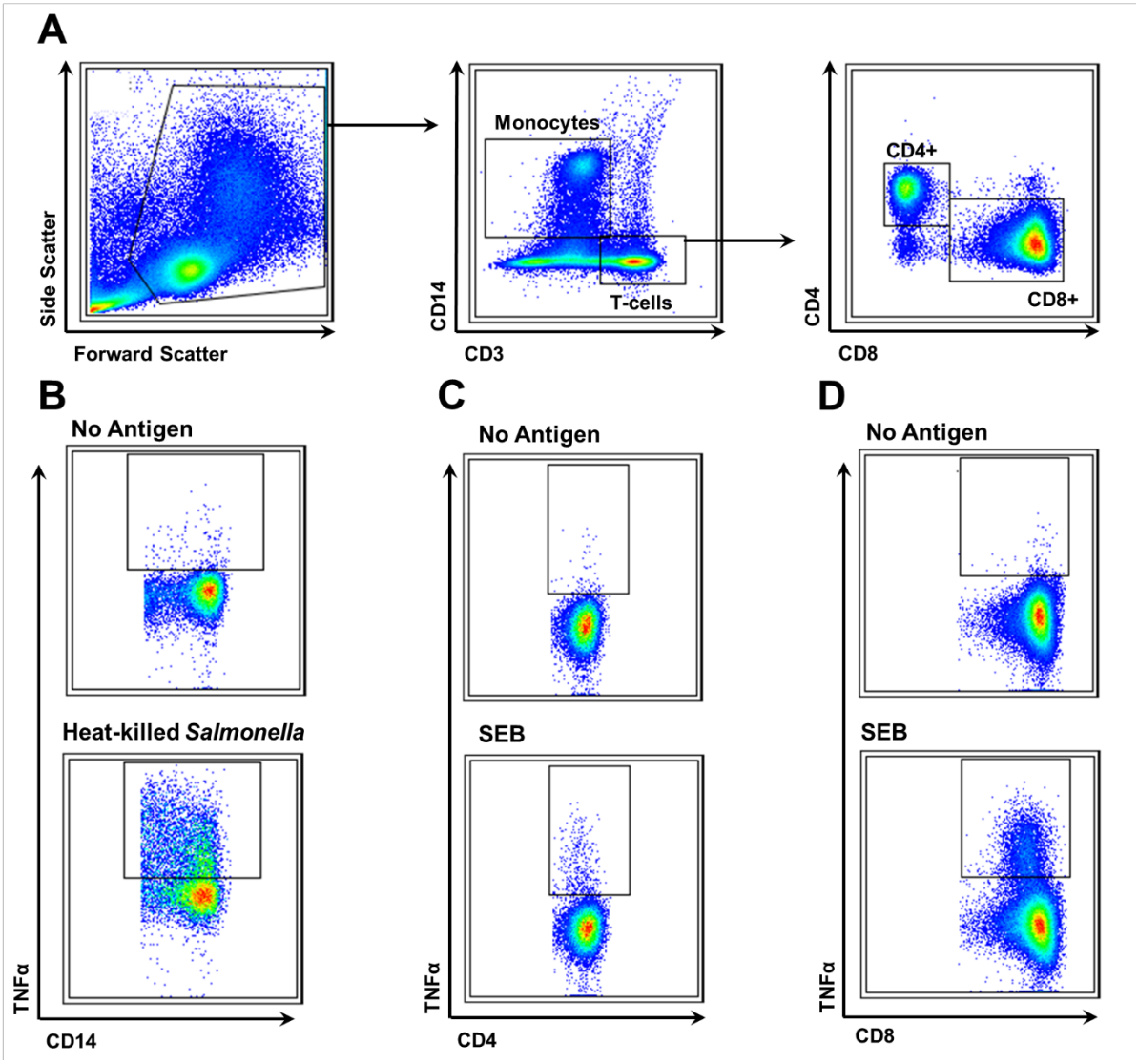

1416

1417 **figure S9. Flow cytometry gating strategy for analysis of monocyte and T-cell**

1418 **intracellular cytokine responses.** (**A**) Flow cytometry gating strategy for identification of

1419 monocytes (CD14+) and T-cells (CD3+, sub-divided by CD4 and CD8 expression) in PBMC

1420 cultured for 6h. (**B**) Flow cytometry gating of TNFα-expressing monocytes after 6h culture

1421 without antigen or with 10^8 cells/mL of heat-killed *Salmonella typhimurium*. Flow cytometry

1422 gating of TNFα-expressing (**C**) CD4+ and (**D**) CD8+ T-cells after 6h culture without antigen

1423 or with 1 μg/mL Staphylococcal enterotoxin B (SEB). Flow cytometry plots are

1424 representative of 24 PBMC cultures conducted without drug treatment.

table S1. Characteristics of HIV-negative and HIV-positive UK adult volunteers

	HIV-	HIV+ ART >2 years	HIV+ ART naïve[1]
n	8	6	10
Gender (M, F)	7, 1	6, 0	8, 2
Age (range)	38 (27-59)	59 (41 -81)	40 (27 - 61)
HIV viral load (copies/mL)	-	<40	17,225 (<40 - 78,318)
CD4 count (cells/mm^3)	-	545 (211-826)	585 (278 - 997)
Years on ART (range)	-	10 (4-17)	-

Mean values are shown.

[1]One participant in group 2 was an 'elite controller' (viral load <40 copies/mL, CD4 count: 723 cells/mm^3); minimum viral load of non-elite controller participants in the HIV+ ART naïve group was 615 copies/mL.

table S2. Details of fluorophore-conjugated antibody combinations used for flow cytometry analysis of PBMC from HIV-negative and HIV-positive adults.

Target	Clone	Isotype	Flurophore	Manufacturer	Catalogue#
Uncultured PBMC Phenotyping Panel					
CD16	3G8	IgG1	Pacific Blue	BioLegend	302032
CD38	HB7	IgG1	BV 510	BioLegend	356612
CD14	M5E2	IgG2a, κ	BV 605	BioLegend	301834
CD3	UCHT1	IgG1, κ	FITC	BioLegend	300406
CD4	OKT4	IgG2b, κ	PE	eBiosciences	12-0048-42
CD8a	SK1	IgG1, κ	PE-Cy7	eBiosciences	25-0087-42
HLA-DR	L243	IgG2a, κ	APC-Cy7	BioLegend	307618
Cultured PBMC Intracellular Cytokine Panel					
CD3	UCHT1	IgG1, κ	Pacific Blue	BioLegend	300431
CD4	OKT4	IgG2b, κ	BV 510	BioLegend	317444
CD14	M5E2	IgG2a, κ	BV 605	BioLegend	301834
TNFα	MAb11	IgG1, κ	PE	eBiosciences	12-7349-81
CD8a	SK1	IgG1, κ	PE-Cy7	eBiosciences	25-0087-42
HLA-DR	L243	IgG2a, κ	APC-Cy7	BioLegend	307618

BV - Brilliant Violet; EF - eBiosciences Fluor; AF - Alexa Fluor